INTERNATIONAL ATOMIC ENERGY AGENCY
UNITED NATIONS EDUCATIONAL, SCIENTIFIC AND CULTURAL ORGANIZATION

INTERNATIONAL CENTRE FOR THEORETICAL PHYSICS
34100 TRIESTE (ITALY) - P.O.B. 586 - MIRAMARE - STRADA COSTIERA 11 - TELEPHONE: 2240-1
CABLE: CENTRATOM - TELEX 460392-I

SMR/291 - 2

SPRING COLLEGE IN CONDENSED MATTER
ON
"THE INTERACTION OF ATOMS AND MOLECULES WITH SOLID SURFACES"
(25 April - 17 June 1988)

BASIC VIBRATIONAL PROPERTIES OF SURFACES

F. GARCIA-MOLINER
Instituto de Ciencia de Materiales
C.S.I.C.
Serrano 123
28006 Madrid
Spain

BASIC VIBRATIONAL PROPERTIES OF SURFACES

by

F. GARCÍA-MOLINER

INSTITUTO DE CIENCIA DE MATERIALES

C.S.I.C.

SERRANO 123

28006 MADRID - SPAIN

INDEX

BASIC VIBRATIONAL PROPERTIES OF SURFACES

by

F. García-Moliner

Instituto de Ciencia de Materiales,

C.S.I.C.,

Serrano 123 — 28006 Madrid — SPAIN

1. Generalities on lattice dynamics

A first principles formulation of the study of lattice vibrations in a crystal would start from the total Hamiltonian

$$H = T_e + T_i + \Phi_{ii}(R) + \Phi_{ee}(r) + \Phi_{ie}(r,R), \qquad (1.1)$$

where T denotes kinetic energy, e electrons, i ions, R ion coordinates and r electron coordinates. For an eigenstate of this system

$$H\Psi(r,R) = E\Psi(r,R). \qquad (1.2)$$

A rigorous solution of this problem entails a formidable task, so we would like to simplify it. We note that ions are of order 10^3 to 10^5 times heavier than electrons, so we may expect their motions to involve sufficiently different time scales that they may be decoupled to a good approximation. It does not seem unreasonable to expect that when the ions move the electrons can follow their motions adiabatically, i.e. that their states are deformed without undergoing abrupt transitions so as to adapt themselves to the instantaneous configuration of ionic positions and so that their interactions can be evaluated as if they "saw" the ions frozen in their instantaneous positions. This is the idea of the Born-Oppenheimer or adiabatic approximation,

in which one imagines some frozen configuration R and writes down the R-dependent Schrödinger equation

$$\left[T_e + \Phi_{ee}(r) + \Phi_{ie}(r,R)\right] \chi_R(r) = E_e(R)\, \chi_R(r) \qquad (1.3)$$

for the electronic system, for which the eigenfunction and the eigenvalue contain the ionic coordinates R as parameters. The task of lattice dynamics is to study the validity of (1.3).

We shall not go into the details of this analysis, which can be found in standard textbooks, but it will be instructive to follow the highlights of such a study just to see the meaning of the approximations involved. Note that $E_e(R)$ includes not only the electron-electron and electron-ion interactions in the presence of the ions, but also the kinetic energy of the electrons and thus also depends on the ion coordinates R. In the spirit of the adiabatic approximation we try

$$\Psi(r,R) = \chi_R(r)\, \psi(R). \qquad (1.4)$$

On substituting this in (1.2) and using (1.3) one finds that for this to be an eigenfunction of H it must be possible (i) to neglect certain terms and (ii) to have $\psi(R)$ satisfy

$$\left[T_i + \Phi(R)\right] \psi(R) = E\, \psi(R), \qquad (1.5)$$

where

$$\Phi(R) = \Phi_{ii}(R) + E_e(R). \qquad (1.6)$$

Note that in the eigenvalue equation for the ionic wavefunction we have introduced the <u>effective potential energy function</u> (1.6) to which the electrons contribute through $E_e(R)$. It turns out that, although due to different reasons, the adiabatic approximation can be usually justified to study lattice dynamics in insulators, semiconductors and metals. The validity of this approximation does not depend on having a weak electron-ion coupling but on whether it is the <u>static</u> or the <u>dynamic</u> aspects of this interaction that mainly intervene in the phenomenon under study. If we want to study simply lattice dynamics as such, i.e. we want to obtain a phonon band structure, then the static aspects of the electron-ion interaction are explicitly included in $\Phi_{ie}(r,R)$ and the issue is decided by the other considerations just outlined. However, this ceases to hold for problems where the electron dynamics is explicitly involved, e.g. superconductivity or ordinary resistivity due to electron-phonon scattering, in which case we must take explicit account of (virtual or real) abrupt transitions between electronic states, the absence of which constitutes the very notion of <u>adiabatic</u> approximation.

Now, in this approximation we are supposed to start from the effective potential $\Phi(R)$ (1.6) for the ionic motions. As noted above, an <u>ab initio</u> calculation of this quantity entails a previous calculation of $E_e(R)$, which is still a major computational task. Thus, in spite of some important simplifications we still have a very substantial job to do. However, the adiabatic argument provides a suggestive hint to the form of (1.5). If we know the type of ion-ion interactions to be expected for a given crystal, then we can start from some appropriate phenomenological model, i.e., we can attempt to design $\Phi(R)$ as a phenomenological potential which contains the appropriate type of interactions, e.g. central forces (two-body interactions), angular forces (three-body interactions), nearest neighbours (NN) or next-nearest neigh-

bours (NNN) interactions, etc. Let R_0 be the equilibrium positions and R the actual positions when the ions are displaced through a displacement $\underline{u} = \underline{R} - \underline{R}_0$. For small displacements we expand

$$\Phi = \Phi_0 + \sum_r f_r u_r + \frac{1}{2}\sum_{rs} f_{rs} u_r u_s + \frac{1}{3!}\sum_{rsp} f_{rsp} u_r u_s u_p + \cdots . \quad (1.7)$$

(We can think of the labels as spanning all ionic positions and spatial coordinates). It suffices to consider succintly the form of Φ. Stopping at the second order terms we have the <u>harmonic approximation</u>. The <u>anharmonic terms</u>, beyond second order, are essential for the study of some phenomena like thermal expansion or thermal conductivity, but the harmonic approximation suffices to study the phonon band structure and thus will be the level of our discussion.

2. Equations of motion and force constants

We now summarise the basic equations which lay out the notation to be employed throughout. Let $\underline{a}_1, \underline{a}_2, \underline{a}_3$ be three linearly independent <u>primitive translation vectors</u> defining a <u>primitive unit cell</u>. We denote the equilibrium position of the l-th unit cell as

$$\underline{r}(l) = l_1 \underline{a}_1 + l_2 \underline{a}_2 + l_3 \underline{a}_3 . \quad (2.1)$$

In <u>primitive</u> or <u>Bravais lattices</u> there is just one atom per unit cell and (2.1) gives the positions of the atoms in the crystal. In general we have s (≥ 1) atoms per unit cell. These form the <u>basis</u> of the crystal structure and we need an inner index k to label the atoms of the basis. The atomic positions in the crystal are then

$$\underline{R}(l,k) = \underline{r}(l) + \underline{r}(k) . \quad (2.2)$$

In fact these -discrete- positions correspond to what we have

termed R_0, the equilibrium positions. The actual ionic positions in the vibrating crystal are

$$\underline{R}(l,k) = \underline{r}(l,k) + \underline{u}(l,k) . \quad (2.3)$$

The task of lattice dynamics is to study $\underline{u}(l,k)$, with components $u_\alpha(l,k)$, $\alpha = x,y,z$. We cast Φ as a function of the instantaneous atomic positions

$$\Phi = \Phi\{\cdots\cdots, \underline{r}(l,k) + \underline{u}(l,k), \cdots\cdots\} \quad (2.4)$$

and expand for small displacements up to second order

$$\Phi = \Phi_0 + \sum_{l\alpha} \Phi_\alpha(l,k) u_\alpha(l,k) + \frac{1}{2}\sum_{\substack{lk\alpha \\ l'k'\beta}} \Phi_{\alpha\beta}(l,k;l',k') u_\alpha(l,k) u_\beta(l',k') , \quad (2.5)$$

where

$$\Phi_\alpha(l,k) = \left[\frac{\partial \Phi}{\partial u_\alpha(l,k)}\right]_0 , \quad (2.6.a)$$

$$\Phi_{\alpha\beta}(l,k;l',k') = \left[\frac{\partial^2 \Phi}{\partial u_\alpha(l,k)\,\partial u_\beta(l',k')}\right]_0 . \quad (2.6.b)$$

The force acting in the direction α on the atom (l,k) for a given system of displacements of all the other atoms is

$$F_\alpha(l,k) = -\frac{\partial \Phi}{\partial u_\alpha(l,k)} = -\Phi_\alpha(l,k) - \sum_{l'k'\beta} \Phi_{\alpha\beta}(l,k;l',k') u_\beta(l',k') . \quad (2.7)$$

Consider all atoms at their equilibrium positions. Then all displacements and forces vanish. Hence

$$\Phi_\alpha(l,k) = 0 , \quad (2.8)$$

so that the harmonic potential is

$$\Phi - \Phi_0 = \frac{1}{2} \sum_{\substack{lk\alpha \\ l'k'\beta}} \Phi_{\alpha\beta}(l,k;l',k') u_\alpha(l,k) u_\beta(l',k') , \qquad (2.9)$$

the force is

$$F_\alpha(l,k) = - \sum_{l'k'\beta} \Phi_{\alpha\beta}(l,k;l',k') u_\beta(l',k') \qquad (2.10)$$

and the equation of motion for the atom (l,k) with mass m_k is

$$m_k \ddot{u}_\alpha(l,k) = - \sum_{l'k'\beta} \Phi_{\alpha\beta}(l,k;l',k') u_\beta(l',k') . \qquad (2.11)$$

The coefficients $\Phi_{\alpha\beta}(l,k;l',k')$ are called the <u>force constants</u>, to be obtained either from empirical fitting, from <u>ab initio</u> calculation or from a combination of hard labour, approximations and fitting.

The force constants satisfy some general relationships. Their complete formal proof is a bit lengthy but it is easy to see what is happening and to obtain quickly the main properties at the expense of accessible informalities:

- The order of differentiation in (2.6.b) can be inverted. Hence

$$\Phi_{\alpha\beta}(l,k;l',k') = \Phi_{\beta\alpha}(l',k';l,k) \qquad (2.12)$$

- Consider a rigid translation of the entire crystal and note that there are three such independent translations. Let this be through a given distance v_β. All associated forces must vanish:

$$\sum_\beta \Big[\sum_{l'k'} \Phi_{\alpha\beta}(l,k;l',k') \Big] v_\beta = 0 \qquad (2.13)$$

for every independent value of v_β ($\beta = x,y,z$). Hence

$$\sum_{l'k'} \Phi_{\alpha\beta}(l,k;l',k') = 0 . \qquad (2.14)$$

It is useful to cast this as

$$\Phi_{\alpha\beta}(l,k;l,k) = - \sum_{(l',k') \neq (l,k)} \Phi_{\alpha\beta}(l,k;l',k') . \qquad (2.15)$$

- Consider a primitive translation $\underline{t}(m) = m_1 \underline{a}_1 + m_2 \underline{a}_2 + m_3 \underline{a}_3$. This carries atom (l,k) to $(l+m,k)$ and (l',k') to $(l'+m,k')$. The interactions cannot be different. Thus

$$\Phi_{\alpha\beta}(l+m,k;l'+m,k') = \Phi_{\alpha\beta}(l,k;l',k') . \qquad (2.16)$$

Take $m = -l$. Then

$$\Phi_{\alpha\beta}(l,k;l',k') = \Phi_{\alpha\beta}(0,k;l'-l,k') \qquad (2.17)$$

and for $m = -l'$:

$$\Phi_{\alpha\beta}(l,k;l',k') = \Phi_{\alpha\beta}(l'-l,k;0,k') . \qquad (2.18)$$

In short: The force constants depend on l and l' only through their difference.

3. Dynamical matrix and eigenvectors

Consider a crystal with N atoms and Born-von Karman periodic boundary conditions. We seek solutions of the form

$$u_\alpha(l,k) = \frac{1}{2\sqrt{N m_k}} \Big\{ A(\underline{q}) e_\alpha(k|\underline{q}) e^{i[\underline{q}\cdot\underline{r}(l,k) - \omega(\underline{q})t]} + \text{c.c.} \Big\} . \qquad (3.1)$$

$\underline{q}$ is the wavevector, $A(\underline{q})$ the amplitude and $\underline{e}(k|\underline{q})$ the polarisation vector. A general vibrational state is a combination of waves like (2.19). Substituting this in (2.11) we obtain the equation of motion in Fourier transform

$$\omega^2(\underline{q}) e_\alpha(k|\underline{q}) = \sum_{k'\beta} D_{\alpha\beta}(\underline{q};k,k') e_\beta(k'|\underline{q}) . \qquad (3.2)$$

This introduces the <u>dynamical matrix</u> $\underline{D}$ of elements

$$D_{\alpha\beta}(\underline{q};k,k') = \frac{1}{\sqrt{m_k m_{k'}}} \sum_{l'} \Phi_{\alpha\beta}(l,k;l',k') e^{-i\{\underline{q}\cdot[\underline{r}(l,k) - \underline{r}(l',k')]\}} \qquad (3.3)$$

Using (2.1), (2.2) and (2.16, 17, 18) $\underline{\underline{D}}$ can be cast as

$$D_{\alpha\beta}(\underline{q};k,k') = \frac{e^{i\underline{q}\cdot[\underline{r}(k')-\underline{r}(k)]}}{\sqrt{m_k m_{k'}}} \sum_L \Phi_{\alpha\beta}(0,k;L,k') e^{i\underline{q}\cdot\underline{r}(L)}, \qquad (3.4)$$

where $L = l' - l$. We recall that $\underline{r}(k)$ gives the position of the k-th atom within one unit cell, while $\underline{r}(L)$ locates the different cells. Thus $\underline{\underline{D}}$ is like a kind of Fourier transform of $\underline{\underline{\Phi}}$, though not quite. Mass factors enter $\underline{\underline{D}}$, due to the inertial term in the equation of motion, and there is only a summation over the primitive lattice, the geometry of the basis remaining explicitly displayed in the prefactor, which depends explicitly on the atomic positions within one unit cell.

The first task is to decide on the model for $\underline{\underline{\Phi}}$. This is physics. Then we must obtain $\underline{\underline{D}}$. This is geometry. Later on we shall see how the dynamical matrix of a given crystal is conveniently cast in a different form in which a 3-D crystal is described as a linear sequence of 2-D atomic layers, the choice being adapted to the crystal orientation of the surface to be studied. For the time being we stick to the 3-D crystal treated as a bulk. We cast (3.2) as

$$\sum_{k'\beta} [\omega^2 \delta_{\alpha\beta}\delta_{kk'} - D_{\alpha\beta}(\underline{q};k,k')]\, e_\beta(k'|\underline{q}) = 0. \qquad (3.5)$$

This is the $3s \times 3s$ matrix representation of an eigenvalue equation: $\underline{e}(k'|\underline{q})$ is the eigenvector and $\omega^2(q)$ the eigenvalue. The secular equation is

$$\det |\omega^2(\underline{q})\delta_{\alpha\beta}\delta_{kk'} - D_{\alpha\beta}(\underline{q};k,k')\, e_\beta(k'|\underline{q})| = 0, \qquad (3.6)$$

an algebraic equation of degree $3s$. For a given $\underline{q}$ there are

in general $3s$ (different or maybe some equal) eigenvalues or branches $\omega_j^2(\underline{q})$ with $j = 1, 2, \ldots, 3s$. It is easily seen that $\underline{\underline{D}}$ is Hermitian, whence the eigenvalues are real and all $\omega_j(\underline{q})$'s are either real or imaginary. The latter would blow up timewise. Thus only real $\omega_j(\underline{q})$'s are physically admissible solutions. Each one gives a branch in the phonon band structure of the crystal.

Having found one eigenvalue we feed it back into (3.5), which can be cast in compact matrix form as

$$\underline{\underline{D}}(\underline{q})\cdot\underline{e}(\underline{q}|j) = \lambda_j(\underline{q})\,\underline{e}(\underline{q}|j), \quad \lambda_j(\underline{q}) = \omega_j^2(\underline{q}). \qquad (3.7)$$

This yields the eigenvectors up to an amplitude factor, which can be chosen to satisfy the <u>orthonormality</u> and <u>closure</u> relations

$$\sum_{k\alpha} e_\alpha^*(k|\underline{q}j)\, e_\alpha(k|\underline{q}j') = \delta_{jj'}, \qquad (3.8a)$$

$$\sum_j e_\alpha(k|\underline{q}j)\, e_\beta^*(k'|\underline{q}j) = \delta_{\alpha\beta}\delta_{kk'}. \qquad (3.8b)$$

It is further seen that

$$e_\alpha^*(k|-\underline{q}j) = e_\alpha(k|\underline{q}j). \qquad (3.9)$$

From (3.7) and (2.14) one can prove that out of the $3n$ branches $\omega_j^2(\underline{q})$ for each given value of $\underline{q}$, there are three which tend to zero as $q \to 0$. These are the <u>acoustic modes</u>. In the limit $q = 0$ they describe the three independent rigid translations of the entire crystal. The other branches (when $n > 1$) correspond to the so called <u>optical modes</u>. Further details and alternative ways to define $\underline{\underline{D}}$ and $\underline{e}$ can be found in standard textbooks. Here we have simply surveyed the main basic facts and laid out the notation to set the stage for eventual studies of surface dynamics.

4. Some practical examples.

It is instructive to work out the details of some force constants models. Appendix A gives an example: Simple cubic lattice, nearest neighbour (NN) and next nearest neighbour (NNN) interactions and central and angular forces. Here we shall consider an f.c.c. lattice with central forces and NN interactions only. This is a very idealised model but it has the virtue that it has a real crystalline lattice and it serves very well to illustrate the main features of the results appearing in an actual surface phonon calculation. We shall see later that sometimes it can even have a reasonable almost quantitative value.

In the f.c.c. lattice there are atoms at the corners and at the face centres of a cube of side a. The rhombohedral unit cell of volume $a^3/4$ contains one atom. Geometrical details are given in Fig. 1. We concentrate on one atom defined as central atom. It has twelve NN. The unit vectors from the central atom to its NN are listed in Fig. 1. Our model is

$$\Phi = \frac{K}{4}\sum_{ll'}\left[\left(\underline{u}_{ll'}\cdot\underline{r}_{ll'}\right)\cdot\underline{r}_{ll'}\right]^2, \qquad (4.1)$$

where $\underline{r}_{ll'}$ is the unit vector of $\underline{r}(l')-\underline{r}(l)$. In this case there is no internal k index (one atom/unit cell). This describes a system of central forces.

The formula for the dynamical matrix (3.4) in this case can be simplified as

$$D_{\alpha\beta}(\underline{q}) = \frac{1}{m}\sum_{\underline{L}} \Phi_{\alpha\beta}(\underline{L})\, e^{i\underline{q}\cdot\underline{L}}, \qquad (4.2)$$

where $\underline{L}_m$ spans, from the origin at the central atom, the position vectors of all twelve NN and also the central atom itself ($\underline{L}=0$). By using (2.15) we can cast (4.2) as

$$D_{\alpha\beta}(\underline{q}) = \frac{1}{m}\sum_{\underline{L}\neq 0} \Phi_{\alpha\beta}(\underline{L})\, e^{i\underline{q}\cdot\underline{L}}. \qquad (4.3)$$

From (4.1) we have

$$\frac{\partial^2\Phi}{\partial u_{l,\alpha}\,\partial u_{l',\beta}} = -\frac{K}{2}\, r_{ll',\beta}\, r_{ll',\alpha}, \quad (l'\neq l). \qquad (4.4)$$

We use this for $l=0$ (central atom) and $\underline{r}_{ll'}$ denoting the $\underline{r}_{0j}$'s listed in Fig. 1. This yields the following non vanishing force constants

$$\Phi_{xx}(1)=\Phi_{xx}(2)=\Phi_{xx}(3)=\Phi_{xx}(4)=\Phi_{xx}(5)=\Phi_{xx}(6)=\Phi_{xx}(7)=\Phi_{xx}(8) = -\frac{K}{4}$$

$$\Phi_{xy}(1)=\Phi_{xy}(2) = -\frac{K}{4} = -\Phi_{xy}(3) = -\Phi_{xy}(4)$$

$$\Phi_{xz}(5)=\Phi_{xz}(6) = -\frac{K}{4} = -\Phi_{xz}(7) = -\Phi_{xz}(8)$$

$$\Phi_{yy}(1)=\Phi_{yy}(2)=\Phi_{yy}(3)=\Phi_{yy}(4)=\Phi_{yy}(9)=\Phi_{yy}(10)=\Phi_{yy}(11)=\Phi_{yy}(12) = -\frac{K}{4}$$

$$\Phi_{yz}(9)=\Phi_{yz}(10) = -\frac{K}{4} = -\Phi_{yz}(11) = -\Phi_{yz}(12)$$

$$\Phi_{zz}(5)=\Phi_{zz}(6)=\Phi_{zz}(7)=\Phi_{zz}(8)=\Phi_{zz}(9)=\Phi_{zz}(10)=\Phi_{zz}(11)=\Phi_{zz}(12) = -\frac{K}{4}$$

$$\Phi_{yx}(l')=\Phi_{xy}(l'); \quad \Phi_{zx}(l')=\Phi_{xz}(l'); \quad \Phi_{yz}(l')=\Phi_{zy}(l').$$

Whence from (4.2), putting $\varphi_\alpha = \frac{a q_\alpha}{2}$

$$D_{xx}(\underline{q}) = \frac{K}{m}\left[\sin^2\frac{(\varphi_x+\varphi_y)}{2} + \sin^2\frac{(\varphi_x-\varphi_y)}{2} + \sin^2\frac{(\varphi_x+\varphi_z)}{2} + \sin^2\frac{(\varphi_x-\varphi_z)}{2}\right]$$

$$D_{xy}(\underline{q}) = \frac{K}{m}\left[\sin^2\frac{(\varphi_x+\varphi_y)}{2} - \sin^2\frac{(\varphi_x-\varphi_y)}{2}\right] = D_{yx}(\underline{q})$$

$$D_{xz}(\underline{q}) = \frac{K}{m}\left[\sin^2\frac{(\varphi_x+\varphi_z)}{2} - \sin^2\frac{(\varphi_x-\varphi_z)}{2}\right] = D_{zx}(\underline{q})$$

$$D_{yy}(\underline{q}) = \frac{K}{m}\left[\sin^2\frac{(\varphi_x+\varphi_y)}{2} + \sin^2\frac{(\varphi_x-\varphi_y)}{2} + \sin^2\frac{(\varphi_y+\varphi_z)}{2} + \sin^2\frac{(\varphi_y-\varphi_z)}{2}\right]$$

$$D_{yz}(\underline{q}) = \frac{K}{m}\left[\sin^2\frac{(\varphi_y+\varphi_z)}{2} - \sin^2\frac{(\varphi_y-\varphi_z)}{2}\right] = D_{zy}(\underline{q})$$

$$D_{zz}(\underline{q}) = \frac{K}{m}\left[\sin^2\frac{(\varphi_x+\varphi_z)}{2} + \sin^2\frac{(\varphi_x-\varphi_z)}{2} + \sin^2\frac{(\varphi_y+\varphi_z)}{2} + \sin^2\frac{(\varphi_y-\varphi_z)}{2}\right].$$

We can now study the eigenvalue problem (3.5), (3.6).
Consider propagation along symmetry directions.
Take $\underline{q} = (q, 0, 0)$. This yields one longitudinal mode

$$\omega_L^2 = D_{xx} = \frac{4K}{m}\sin^2\frac{aq}{4} \qquad (4.5)$$

and two degenerate transverse modes

$$\omega_{T_1}^2 = \omega_{T_2}^2 = D_{yy} = D_{zz} = \frac{2K}{m} \sin^2 \frac{aq}{4} \quad . \tag{4.6}$$

Take $\underline{q} = \frac{1}{\sqrt{2}}(q,q,0)$. Then $D_{xz} = D_{yz} = 0$ but $D_{xy} \neq 0$. Thus one decoupled transverse solution is

$$\omega_{T_2}^2(q) = D_{zz} = \frac{4K}{m} \sin^2 \frac{aq}{4\sqrt{2}} \quad , \tag{4.7}$$

corresponding to a vibration in the $\underline{x}$ direction. For the rest we have a 2x2 dynamical matrix with

$$D_{xx} = D_{yy} = \frac{K}{m}\left[\sin^2 \frac{aq}{2\sqrt{2}} + 2 \sin^2 \frac{aq}{4\sqrt{2}}\right] ; \qquad D_{xy} = D_{yx} = \frac{K}{m} \sin^2 \frac{aq}{4\sqrt{2}} \tag{4.8}$$

This 2x2 secular problem has the two roots

$$\omega_{\pm}^2 = D_{xx} \pm D_{xy} \quad . \tag{4.9}$$

The + sign corresponds to the normalised eigenvector $\underline{e}_L = \frac{1}{\sqrt{2}}(1,1,0)$, which describes a longitudinal mode with

$$\omega_L^2 = \omega_+^2 = \frac{2K}{m}\left[\sin^2 \frac{aq}{2\sqrt{2}} + \sin^2 \frac{aq}{4\sqrt{2}}\right] . \tag{4.10}$$

The other root is a transverse mode (T_1) with normalised eigenvector $\underline{e}_{T_1} = \frac{1}{\sqrt{2}}(-1,1,0)$ and eigenvalue

$$\omega_{T_1}^2 = \omega_-^2 = \frac{2K}{m} \sin^2 \frac{aq}{4\sqrt{2}} \quad . \tag{4.11}$$

The normalised eigenvector of (4.7) is obviously $\underline{e}_{T_2} = (0,0,1)$.

If instead of this we study propagation in the (1,1,1) direction then we also find three eigenvectors independent of $\underline{q}$. However, for any other $\underline{q}$ not in a symmetry direction the eigenvectors depend on both the modulus and the direction of $\underline{q}$. For future reference let us keep in mind this simple picture corresponding to propagation in a (1,0,0) and a (1,1,0) direction (Fig. 2)

5. The layer description of lattice dynamics

In order to prepare the description of the bulk for an eventual study of the surface problem it is convenient to single out the plane orientation which the surface will eventually have and to let $L = (l_1, l_2) = (l, m)$ label two-dimensional (2-D) atomic positions within an atomic layer with this orientation while n labels the successive layers. We then redefine the basis vectors, if necessary, so that $\underline{a}_1$ and $\underline{a}_2$ are in the plane $\underline{n}$ = const., while $\underline{a}_3$ is perpendicular to this. This is the appropriate geometry for the eventual study of the surface. For the time being we are interested in outlining the corresponding layer description of the bulk. For instance, instead of writing $\Phi_{\alpha\beta}(l,l')$ or $\Phi_{\alpha\beta}(l,k;l',k')$ as in §2, where l is an abbreviated notation for the full 3-D (l,m,n), we write

$$\Phi_{\alpha\beta}(L,L';n,k,n',k') = \frac{\partial^2 \Phi}{\partial u_\alpha(L,nk)\partial u_\beta(L',n'k')} \quad . \tag{5.1}$$

We stress that the meaning of L here is not the same as in §4. By repeating in the 2-D plane the arguments of the 3-D bulk we find that (5.1) depends on L and L' only through their difference and

$$\Phi_{\alpha\beta}(L-L';n,k,n',k') = \Phi_{\beta\alpha}(L'-L;n',k',n,k) \tag{5.2}$$

(This is only a consequence of the 2-D periodicity and will also hold if the crystal is cut in half). There are other important properties of the bulk which is convenient to cast in layer notation. The two basic ones are translational invariance

$$\sum_{L',n',k'} \Phi_{\alpha\beta}(L-L';n,k,n',k') = 0 \qquad (5.3)$$

and <u>rotational invariance</u>

$$\sum_{L',n',k'} [\Phi_{\alpha\beta}(L-L';n,k,n',k') r_\gamma(L';n',k') - \Phi_{\alpha\gamma}(L-L';n,k,n',k') r_\beta(L';n',k')] = 0 \qquad (5.4)$$

The proof of (5.4) is a bit more involved but here we merely quote the results. The point is that these invariance conditions do not depend on any particular details of the symmetry group of the crystal. They must hold in all cases, even for any group of atoms, since they simply express the fact that no forces can be created when any array of atoms is bodily translated or rotated or displaced in any way as long as it is a rigid bodily motion of the entire group of atoms. These invariance conditions play an important role in some formulations of surface lattice dynamics (a significant case will be referred to in §11) and are of fundamental importance for a correct description of the long wave (elastic) limit.

Now, the equation of motion in the layer description reads

$$m_k(n)\, \ddot{u}_\alpha(L;n,k) = -\sum_{L',n',k',\beta} \Phi_{\alpha\beta}(L-L';n,k,n',k') u_\beta(L';n',k') \qquad (5.5)$$

At this stage we Fourier transform in 2-D, introducing the 2-D wavevector $\underline{K}$, conjugate to the 2-D position $\underline{r}(L)$. The normal mode analysis of (5.5) then rests on waves of the form

$$\underline{u}(\underline{r};n,k) = \frac{1}{2\sqrt{N_s m_k(n)}}\, \underline{\hat{e}}(n,k|\underline{K},j)\, e^{i[\underline{K}\cdot\underline{r} - \omega_j(\underline{K})t]}, \quad \underline{r} = \underline{r}(L), \qquad (5.6)$$

where N_s is the number of unit cells in the 2-D lattice, i.e., the

number of values that L takes, and we use the 2-D periodic Born-von Karman boundary conditions. Note that here we are using the alternative definition of the polarisation vectors

$$\underline{\tilde{e}}(n,k|\underline{K},j) = e^{i\underline{K}\cdot\underline{r}(k)}\, \underline{e}(n,k|\underline{K},j) \qquad (5.7)$$

The secular system corresponding to (5.6) is

$$\omega_j^2(\underline{K})\, \tilde{e}_\alpha(n,k|\underline{K},j) = \sum_{n',k',\beta} D_{\alpha\beta}(n,k,n',k';\underline{K})\, \tilde{e}_\beta(n',k'|\underline{K},j), \qquad (5.8)$$

where

$$D_{\alpha\beta}(n,k,n',k';\underline{K}) = \frac{1}{\sqrt{m_k(n)\, m_{k'}(n')}} \sum_{L'} \Phi_{\alpha\beta}(L-L';n,k,n',k')\, e^{i\underline{K}\cdot[\underline{r}(L)-\underline{r}(L')]} \qquad (5.9)$$

Note that for this dynamical matrix only the 2-D wavevector $\underline{K}$ is introduced and explicit layer indices are displayed.

So far this is a mere rewriting of the bulk lattice dynamics in layer notation. In spite of the 2-D character emphasised by these equations the problem remains 3-D, only that (5.6), for instance, displays explicitly the harmonic form of the wave only in 2-D. If the actual wavevector is equal to $\underline{K}$, then the $\underline{n}$-dependent quantities appearing in (5.6) have the same value for all $\underline{n}$. This would then amount to a standard description, with $\underline{n}$ omitted, of a 3-D bulk wave which happens to travel with $\underline{q} = \underline{K}$. If the wave travels at an angle with the planes $\underline{n} = \text{const.}$, then (5.6) has an $\underline{n}$-dependence which would have to be determined. The layer description would then be very clumsy. The only natural thing to do would be in this case to carry on with the complete Fourier transform for the third spatial component, which would lead us back to the scheme of §4.

The layer description is set up to study the surface problem, for which the layer representation constitutes a natural language as there is an explicit reference to the atomic layers. We expect to find a different situation as we study first the surface and then the successive layers, moving down to the bulk. Before going into this it helps to have a quick look at the long wave limit.

6. Surface waves: A summary of the long wave limit

Consider a bulk, isotropic, elastic medium. It has two degenerate transverse modes ω_T and one longitudinal mode ω_L, with

$$\omega_T = v_T q \;, \quad \omega_L = v_L q \qquad (6.1)$$

Now consider the planes $z = \text{const.}$ and define the vector $\underline{q}$ as $(\underline{\kappa}, q_z)$, where $\underline{\kappa}$ is the projection of $\underline{q}$ on the said planes. Consider a bulk branch $\omega = vq$ (Fig. 3). Take a fixed value κ' of the κ projection of $\underline{q}$ and let q_z grow with this fixed κ'. For $q_z = 0$ the value of ω is $\omega' = v\kappa'$ (a). As q_z grows, so do mod $\underline{q} = q$ and ω, i.e.,

$$q = \sqrt{\kappa^2 + q_z^2} \;; \quad \omega = vq \qquad (6.2)$$

For instance, for $\underline{q}'_1$ (b) we move in (a) to the right of κ', i.e., we move to higher frequencies. If we plot this in (c) we obtain a point like (q'_1). Now increase (6.2) to the value corresponding to $\underline{q}'_2$ (b). We have an even higher frequency (q'_2) in (c). If the tip of $\underline{q}$ varies continuously along the line from $\underline{q}'_1$ to $\underline{q}'_2$, then we generate a vertical line in the (c) diagram which starts from $\omega = \omega'$. Repeat the same process for another value κ''. In the (c) diagram we generate another

vertical line of points starting from $\omega = \omega''$. All these points correspond to the bulk modes. When we vary κ continuously we generate the shaded area of the diagram (c). This describes the same spectrum as (a) but presented in a different manner which emphasises a preferred orientation, something like a continuum counterpart of the layer description of bulk lattice dynamics. If we do this for all the branches of the spectrum, i.e., just for $\omega_L(\underline{q})$ and $\omega_T(\underline{q})$ in this case, then we have a projection of the bulk band structure, this projection being referred to a given orientation. Clearly we have prepared the description of the bulk for the study of surface waves. Now, what do we find when the medium is cut in half, so a free surface with the specified orientation is created? Fig. 4. shows the well known Rayleigh mode which appears below the lowest bulk band threshold. This is a new surface mode, made possible by the change in boundary conditions. Indeed this is a usual way to find this type of solution. One writes down a trial form of the solution of the equations of motion for elastic waves, which contains some parameters. These are determined by imposing the surface boundary conditions and this yields the Rayleigh mode [1]. But this is not all. Let us think in terms of a change in the mode density. Not only a new (surface) mode appears, but also the bulk modes are affected, as all solutions must obey the new boundary conditions. If we look at Fig. 4 and draw a vertical line corresponding to a fixed κ, then the new local value $\mathcal{N}_s(\kappa, \omega)$ of the fixed-κ mode density as a function of ω, projected at the surface, looks like the picture shown in Fig. 5. The two key features of this qualitative picture are (i) the presence of the δ-function peak $\delta(\omega - \omega_R)$, which sig-

mals the existence of the Rayleigh mode and (i) the characteristic humps near the bulk thresholds, where $N_s(\kappa,\omega)$ looks very different from the bulk homogeneous value $N(\kappa,\omega)$. Frequencywise the distortion of the bulk modes piles up near the band edges. Spacewise it tends to accumulate near the surface, as is intuitively obvious. The surface spectrum can be determined by surface Brillouin scattering spectroscopy. Fig. 6 shows experimental results for polycrystalline Al. The incoming probe (a photon) undergoes inelastic scattering in which it exchanges some energy (frequency) and momentum (wavevector) parallel to the surface. These are, respectively, the ω and $\underline{\kappa}$ of the surface mode absorbed or emitted in the inelastic scattering event. It is also intuitively obvious that the scattering cross section must be essentially proportional to the density of modes to be emitted or absorbed. Fig. 6 also shows a theoretical calculation [3] of $N_s(\kappa,\omega)$, in very good agreement with experiment.

This discussion bears out two important points: (i) When the surface is excited it is not only the surface modes but the entire lattice dynamics that is involved. (ii) We have just seen the relevance of an important concept, namely, $N_s(\underline{\kappa},\omega)$. This is an example of a spectral function, a concept to which we shall return in § 11.

In the example of Fig. 6 the calculation was done for an isotropic average of Al, but crystal anisotropy is actually important [4]. In general the two transverse thresholds split apart. Let us plot this in the following manner. First consider, for instance, a continuous elastic but anisotropic medium with cubic symmetry. Consider the (0,0,1)

surface and repeat an analysis similar to that leading to Fig. 3(d) but this time plotting the phase velocity instead of the frequency. Consider bulk waves with $\underline{q} = (\kappa, 0, 0)$. As we saw in § 4, the two transverse modes are degenerate for $\underline{q}$ in this high symmetry direction. Thus the two transverse bulk thresholds are equal. Above this threshold we have bulk modes with the same surface projection $\underline{\kappa} = (\kappa, 0)$ of $\underline{q}$ and somewhere above there is a longitudinal threshold. Now, starting from the (1,0,0) direction tilt the direction of $\underline{\kappa}$ (Fig. 7) so it forms an angle θ with (1,0,0). Then the two transverse thresholds split apart. If we represent this in terms of phase velocities (Fig. 8), then $T_2 = T_2$ for $\theta = 0$ and, as θ increases, one of the two thresholds (T_2) remains constant while the other one (T_1) varies. For some materials $T_1 > T_2$ and for others $T_1 < T_2$ [1,4]. The latter are more interesting. We rotate the (x,y,z) axes so $\underline{x}$ is always the propagation direction (that of $\underline{\kappa}$), $\underline{y}$ is transverse horizontal (parallel to the surface) and $\underline{z}$ is transverse vertical (perpendicular to the surface). Consider $\underline{\kappa}$ in the (1,0,0) direction, $\theta = 0$. Then T_1 is transverse horizontal, with amplitude $(0, u_y, 0)$, T_2 is transverse vertical, with $(0,0,u_z)$ and the L (longitudinal) mode, higher above in Fig. 8, has amplitude $(u_x, 0, 0)$. Below T_2 we have the surface Rayleigh mode. This, as is well known, has sagittal polarisation $(u_x, 0, u_z)$. For increasing θ, R moves typically as shown in Fig. 8 and, at the same time, its polarisation changes gradually so that its sagittal strength decreases while it develops an increasing transverse horizontal amplitude u_y [4]. For $\theta = 45°$, when

we reach the (1,1,0) direction, the sagittal amplitude has decreased to zero while u_y has reached its full value and the surface mode has become degenerate with the T_2 threshold. For this reason this is usually termed a Generalised Rayleigh (GR) mode. Thus for $\theta = 45°$ this has ceased to exist as a surface mode. However another surface mode appears, above T_1 and T_2, which is purely sagittal, like R for $\theta = 0$. This is actually a distinct surface mode, but only for $\theta = 45°$. As θ decreases the sagittal strength decreases and this mode, usually termed a Pseudo Surface Wave (PSW), develops an increasing horizontal transverse amplitude u_y of increasing strength until, for $\theta = 0$, all sagittal strength vanishes and this becomes degenerate with the lowest bulk threshold again. The behaviour of PSW is the opposite to that of R. But this mode has a new feature. For any arbitrary θ it is coupled to the bulk modes (not surprisingly, since it is immersed in the bulk continuum). This means that there is some leakage, i.e., energy from this mode is radiated into the bulk. For real κ the frequency eigenvalue ω is complex, corresponding to a finite lifetime (decay) of the mode. For real ω it is κ that is complex, corresponding to a damping of the mode in its spatial propagation. Technically the so called PSW is in fact a resonance which in practice tends to be a very sharp one (typically the imaginary part is of order 10^{-4} times the real part), i.e., sufficiently long lived that it shows up in the experiments. And, in particular, the imaginary part strictly vanishes for $\theta = 45°$. The so called PSW is then a true surface state which in the language of scattering theory could be called a virtual surface state. Finally, we have referred only to the surface mode solutions but, of course, there are also threshold effects and distortions of the bulk

continuum, as in the isotropic case, only that they are more complicated [5].

From this quick overview of some well known facts for elastic waves (the long wave part of the phonon spectrum) we have learnt (i) that surface dynamics means more than simply surface modes, (ii) that crystalline anisotropy is important and (iii) that even referring only to surface modes we must anticipate also the possibility of other solutions of resonant type. The elasticity limit, describing only the long wave part, gives a limited picture. It is clear that the projection of the bulk phonon band structure and the different kinds of solutions and effects will show up in a more complicated pattern. However, the basic principles are the same; it is the details that differ and these can only be found by explicit calculation for each case.

7. Surface phonon calculations

Let us return to the dynamical matrix of a crystal cast in the layer notation (5.9). For fixed $\underline{n}$ and $\underline{n}'$ this is a $3s \times 3s$ matrix. Now suppose that instead of an infinite crystal we have a finite slab containing N_L atomic layers. Then the n-dependence becomes an explicit feature of the problem. To begin with, for the force constants themselves. The forces acting on the surface atoms are obviously different. At the very least the outer neighbours are missing and we must account for this by 'cutting the links'. This is sometimes described as introducing a 'cleavage perturbation'. Besides, there may also be other changes in these force constants due, for instance, to surface relaxation and/or reconstruction. It is also conceivable that these perturbations may affect one or more atomic layers. All these details should be sorted out in some way or other but when we are finished with this we are left in (5.9)

with a $3sN_L \times 3sN_L$ matrix. What is done in the often practised slab calculations is just to set up the eigenvalue problem for all the N_L atomic layers contained in the slab, simultaneously. I.e. to use precisely this inhomogeneous n- and n'-dependent $3sN_L \times 3sN_L$ dynamical matrix to form the corresponding secular system and then look for the eigenvalues of its determinant and associated eigenvectors. The solutions thus obtained may also exhibit an n-dependence, but this can be very different for the different eigenmodes of the system. There are modes with amplitudes extending across the slab which form different branches which get closer together as N_L increases. For $N_L \to \infty$ these would span the projection of the continuum of the bulk phonon band structure. Others have amplitudes localized near the surface and stay as distinct branches outside the bulk bands. These are identified as surface modes. Frequencywise they may appear within the projection of the bulk spectrum and they may couple to bulk modes, though this is not necessarily implied. Fig. 9 shows an example of results of this type of calculation [6]. In this case the calculations include surface relaxation, but this is not too significant. The purpose of this discussion is not to analyse all details but just to have an idea of what real calculations look like and to discern some general features. Look, for example, at the surface modes for $\bar{E}$ on the segment $\bar{X}\bar{M}$ of the 2D Brillouin Zone: These are well identified and they correspond to short wave phonons. Now move from either $\bar{X}$ or $\bar{M}$ towards $\bar{\Gamma}$, i.e. towards longwaves. As we get near $\bar{\Gamma}$ ($\kappa = 0$), the Rayleigh mode ceases to be well obtained in this calculation. The point is that long waves penetrate a far distance into the bulk and eventually the

two surfaces are coupled. If the two surfaces are very far away, then distinct surface modes are doubly degenerate (assuming inversion symmetry), with only one well defined eigenvalue. If the two surfaces become significantly coupled, then the degeneracy is lifted and the method ceases to be practical. One cannot increase indefinitely the number of atomic layers in the slab because the secular matrix becomes bigger and bigger (Ten to twenty layers are usually employed. Fifteen layer slabs were used for the calculations of Fig. 9). Note also that only the long wave regions, and only for low frequencies (acoustic modes) the projection of the bulk bands looks more or less like Fig. 4. Elsewhere the picture for a real crystal is much more complicated, as is to be expected, with optical modes at higher frequencies and with 'windows' of forbidden bulk frequencies where more surface modes can appear (see also Figs. 10 and 12 through 15). From the discussion at the end of § 6 we may also expect to find resonances. Because of their coupling to bulk modes, the resonances also penetrate far into the bulk and again these tend to be elusive in this type of calculation, in spite of quite considerable efforts made to try and obtain them.

Thus slab calculations are in practice very useful to obtain (albeit at the expense of considerable computation) distinct surface phonon bands, but they have practical shortcomings when resonances or long wave acoustic modes are involved.

Slab calculations are very frequent but of course there are many more methods [7-13]. However, the purpose of these notes is not to review all these methods but to introduce some general concepts in lattice dynamics for which, for reasons to be seen later, it proves convenient to formulate the problem in terms of Green functions.

8. Lattice dynamics in terms of Green functions

Let $R, R', \ldots$ denote 3-D atomic positions in a lattice and cast the force constants matrix in concise form as $\langle R|\underline{\Phi}|R'\rangle$, so the force acting on the atom at R is

$$\langle R|\underline{f}\rangle = -\langle R|\underline{\Phi}\cdot\underline{u}\rangle = -\sum_{R'}\langle R|\underline{\Phi}|R'\rangle\cdot\langle R'|\underline{u}\rangle \qquad (8.1)$$

The various details like contracted products – e.g. $\underline{\Phi}\cdot\underline{u}$ –, etc will be implicitly understood everywhere. The equation of motion is then

$$\langle R|(\underline{\Phi}-\underline{\Omega})\,\underline{u}\,|R'\rangle = 0 \qquad \underline{\Omega} = \underline{M}\,\omega^2 \qquad (8.2)$$

Note: (i) Here we use ω^2 as the natural variable, as it appears naturally in the inertial terms $\ddot{u}$. (ii) We have introduced a diagonal mass matrix $\underline{M}$, meaning that different atoms may have different mass. This situation may arise in the bulk if we have more than one atom/unit cell and also in surface problems if we have an adsorbed layer, so it is convenient to stress the mass factor explicitly. The meaning of the mass matrix is that $\langle R|\underline{M}|R\rangle$ is the mass m_R of the atom at R and the corresponding eigenvalue is $m_R\omega^2$. We then define the Green function $\underline{G}$ (a matrix) associated with (8.2), by

$$\langle R|(\underline{\Phi}-\underline{\Omega})\,\underline{G}\,|R'\rangle = \underline{\delta}(R-R') \qquad (8.3)$$

Thus $\langle R|\underline{G}|R'\rangle$ gives at R the vibration amplitude due to a standard unit input at R'. To put it intuitively, if we wiggle an atom at R', then $\langle R|\underline{G}|R'\rangle$ describes the propagation of this vibration from R' to R. Thus G is a propagator or dynamical response function for lattice vibrations. We can cast (8.3) in concise form as

$$(\underline{\Phi}-\underline{\Omega})\cdot\underline{G} = \underline{I}\,, \qquad (8.4)$$

where $\underline{I}$ is the unit of the complete space of all atoms linked by the force constants contained in $\underline{\Phi}$. The normal mode eigenvalues are the zeros of $\underline{\Phi}-\underline{\Omega}$, i.e., the poles of its inverse $\underline{G}$.

From now on we write all matrices $\underline{G}$, etc, as G, etc. In concise form G has the spectral representation

$$G(\Omega) = \sum_i \frac{|i\rangle\langle i|}{\Phi_i - \Omega} \qquad (8.5)$$

Putting $\Omega = \Omega^+ = \lim_{\varepsilon\to 0}(\Omega + i\varepsilon)$ for a causal description and using

$$\frac{1}{x+i\varepsilon} \to \mathcal{P}\frac{1}{x} - i\pi\delta(x) \qquad (8.6)$$

we have

$$\mathrm{Im}\,G(\Omega^+) = \pi\sum_i |i\rangle\langle i|\,\delta(\Phi_i - \Omega) \qquad (8.7)$$

With an orthogonal basis

$$\mathrm{Im}\sum_i \langle i|\,G(\Omega^+)\,|i\rangle = \mathrm{Im}\,\mathrm{Tr}\,G(\Omega^+) = \pi\sum_i\sum_j \delta_{ij}\delta_{ji}\,\delta(\Phi_j-\Omega) =$$

$$= \pi\sum_i \delta(\Phi_i - \Omega) \qquad (8.8)$$

Now, consider the mode density $N(\Omega)$. By definition

$$\int_1^2 d\Omega\, N(\Omega) \qquad (8.9)$$

is the number of eigenvalues in the interval $(1,2)$. But this can also be expressed as

$$\int_1^2 d\Omega \sum_i \delta(\Phi_i - \Omega)\,, \qquad (8.10)$$

whence

$$N(\Omega) = \frac{1}{\pi}\,\mathrm{Im}\,\mathrm{tr}\,G(\Omega^+)\,. \qquad (8.11)$$

The derivation just given is very unformal, but the result (8.11) is correct, quite general and very important. Note, incidentally, that (8.11) defines a mode density in the variable $m\omega^2$. It is immediate to change this into a density $N(\omega)$ by simply multiplying $N(\Omega)$ by $d\Omega/d\omega = 2m\omega$. Oftentimes the natural variable Ω is defined as ω^2, without mass factor. All these optional definitions entail corresponding different defi-

nitions of the dynamical matrix and all these details are inessential. The (26
point is that (8.11) makes G very useful: The spectrum of the system is contained in the singularities of G. Its poles yield the eigenvalues and (8.11) yields the mode density. $N(\Omega)$ is another example of a spectral function.

9. Surface dynamics in terms of Green functions

Consider now a semi-infinite crystal with a free surface. We assume we have an appropriate force constants model embodied in Φ_s, which includes the interactions between the atoms in the half crystal, the effects of termination, possible surface changes in the force constants between existing atoms at or near the surface and perhaps also other 'surface perturbations' due to relaxation and/or reconstruction. Let I_s be the unit of the half crystal. We want to know G_s, the Green function of the half crystal, defined by

$$(\Phi_s - \Omega)\, G_s = I_s \qquad (9.1)$$

There are many different ways to find G_s. We shall summarise here the basics of one method which can be found in detail in [14] or, with a different presentation designed for a different purpose, in [15].

In a bulk crystal the propagator $\langle R|G|R'\rangle$ can be pictured as a line going from R' to R. However in the presence of a surface it can also be reached by propagation to the surface, reflection and then propagation again, as shown in the picture.

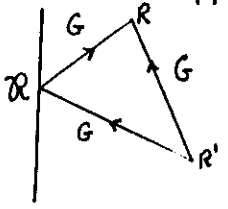

Thus the form of G_s can be expressed as

$$\langle R|G_s|R'\rangle = \langle R|G|R'\rangle + \langle R|G\,\mathcal{R}\,G|R'\rangle, \qquad (9.2)$$

meaning that $\mathcal{R}$ is some surface object which describes reflection. We may convene to cast this in concise form as

$$G_s = G + G\,\mathcal{R}\,G \qquad (9.3)$$ (27

on the understanding that only atomic positions inside the existing half crystal intervene in this and all subsequent formulae. It is important to remember this point.

As seen in § 5, a layer description is convenient to study surface problems. Thus we imagine everything Fourier transformed in 2-D and (9.2) then reads

$$\langle n|G_s|n'\rangle = \langle n|G|n'\rangle + \sum_{s,s'} \langle n|G|s\rangle\langle s|\mathcal{R}|s'\rangle\langle s'|G|n'\rangle \qquad (9.4)$$

Wherever not explicitly shown the $(\underline{k},\Omega)$-dependence is to be understood everywhere. Here s denotes the atomic layers forming the surface domain. By definition this consists of the layers affected by the creation of the surface. Thus the surface domain may (and usually does) contain more than one atomic layer. Let $\mathcal{I}$ denote the projector of the surface domain. We use script characters for all the surface objects which result either from direct definition, like $\mathcal{R}$, or from projection of a bulk object onto the domain $\mathcal{I}$. An object like $\mathcal{R}$ or $\mathcal{G}$ is identically $\mathcal{I}R\mathcal{I}$ or $\mathcal{I}G\mathcal{I}$, but $\mathcal{I}$ will not be explicitly displayed unless it is necessary for clarity. Two especially important surface objects are $\mathcal{G}_s$ and $\mathcal{G}$, the surface projections of G_s, the Green function we want to find, and G, the bulk Green function we are supposed to know. If there are ν_s atomic layers in the surface domain, then $\mathcal{I}$ is the diagonal $3\nu_s \times 3\nu_s$ unit matrix and $\mathcal{R}$, $\mathcal{G}_s$, $\mathcal{G}$ and similar objects are $(\underline{k},\Omega)$-dependent $3\nu_s \times 3\nu_s$ matrices. Their inverses, defined within the subspace of $\mathcal{I}$, satisfy

$$\mathcal{G}_s^{-1}\mathcal{G}_s = \mathcal{G}^{-1}\mathcal{G} = \mathcal{I} \qquad (9.5)$$

The idea of a formulation of this kind is to project the problem in the space of $\mathcal{I}$ and then do there all the relevant algebra, a substan-

tially different philosophy from that of slab calculations. To put it intuitively: We know what happens in the bulk. We want to know what happens in the semiinfinite crystal and we hope that this can be achieved if only we know what happens in the surface domain. Indeed (9.3), or (9.4), says that if we can find R then we know the entire G_s. Thus it all hinges on finding R, and we aim at doing this by means of an algebra to be carried out in the domain having as unit

$$\mathcal{I} = \sum_s |s\rangle\langle s| \qquad (9.6)$$

Now, from (9.3) we have the surface projection

$$G_s = g + g R g, \qquad (9.7)$$

whence

$$R = g^{-1}(G_s - g)\, g^{-1} \qquad (9.8)$$

and, putting this back in (9.3):

$$G_s = G + G g^{-1}(G_s - g)\, g^{-1} G, \qquad (9.9)$$

which expresses the same idea more emphatically: <u>In order to know the complete G_s it suffices to know its surface projection G_s</u>.

Note, in particular, that the new surface modes must be those singularities of (9.9) which are not bulk modes, and these can only come from G_s, so that the zeros of its inverse are the surface mode eigenvalues, i.e., the secular equation is

$$\det |\, G_s^{-1}(\underline{k}, \Omega)\,| = 0. \qquad (9.10)$$

The argument is again very informal but the result (9.10) can be rigorously proved. The point is that here we have a secular equation and the size of the secular matrix is only that of the surface domain. Whether the surface modes penetrate more or less into the bulk is immaterial. A resonance appears as a complex eigenvalue but neither this nor the long waves present any essential difficulty. In fact the elastic limit

can be explicitly recovered as the long wave limit of this analysis [14].

Now, in order to find G_s we go back to (9.1) and take the surface projection

$$\Omega G_s - \mathcal{I}\Phi_s G_s \mathcal{I} = \mathcal{I}. \qquad (9.11)$$

whence

$$G_s^{-1} = \mathcal{I}(\Omega - \Phi_s G_s)\mathcal{I}\, g^{-1}. \qquad (9.12)$$

Take the surface projection of (9.9) <u>from the right only</u>. Then

$$G_s \mathcal{I} = G g^{-1} G_s. \qquad (9.13)$$

The meaning of this is that the matrix element between any layer $\underline{n}$ and a surface layer $\underline{s}$ is

$$\langle n|\, G_s |s\rangle = \sum_{s',s''} \langle n|\, G |s'\rangle\langle s'|\, g^{-1}|s''\rangle\langle s''|\, G_s |s\rangle. \qquad (9.14)$$

For (9.17) we need $G_s G_s^{-1}$ which, on explicit layer representation, is

$$\sum_{s'} \langle n|\, G_s |s'\rangle\langle s'|\, G_s^{-1}|s\rangle = \sum_{s'} \langle n|\, G |s'\rangle\langle s'|\, g^{-1}|s\rangle, \qquad (9.15)$$

i.e.

$$G_s G_s^{-1} = G g^{-1}. \qquad (9.16)$$

Thus

$$G_s^{-1} = \mathcal{I}\Omega - \mathcal{I}\Phi_s G g^{-1}. \qquad (9.17)$$

The important difference between (9.12) and (9.17) is that G_s has disappeared altogether: (9.17) is a <u>formula</u>. It is the formula for G_s we were looking for. From this, as we have just seen, we can obtain directly the surface mode secular equation or evaluate the complete G_s, which contains <u>all</u> the physical information on the semiinfinite crystal.

Now, in §6 we saw the importance of another spectral function, namely the surface projection of the fixed $\underline{k}$ mode density. In a crystal we may have more than one atomic layer, so that

$$\mathcal{N}_s(\underline{k}, \Omega) = \frac{1}{\pi} \mathrm{Im}\, \mathrm{Tr}\, G_s(\underline{k}, \Omega^+) = \frac{1}{\pi} \mathrm{Im} \sum_s \mathrm{tr} \langle s|\, G_s(\underline{k}, \Omega^+)|s\rangle. \qquad (9.18)$$

Here $\underline{\mathrm{tr}}$ means the summation over the three diagonal (x,x), (y,z) and (z,z) terms, i.e., the contributions from all possible polarisations, which can be separately identified if desired. In practice the most interesting local

spectral function is just the projection on the terminal atomic layer (30
with index $\underline{s} = \underline{n} = 0$. We shall indicate this by

$$\rho_s(\underline{k}, \Omega) = \frac{1}{\pi} \mathrm{Im}\, \mathrm{tr} \langle 0 | \mathcal{G}_s(\underline{k}, \Omega^+) | 0 \rangle . \qquad (9.19)$$

This is the discrete crystal analogue of $\mathcal{N}_s(\underline{k}, \Omega)$ (§6). The study of this spectral function provides among other things (see §11) an alternative way to calculate surface phonon dispersion relations. For fixed $\underline{k}$ the values of Ω corresponding to surface modes are those at which $\rho_s(\underline{k}, \Omega)$ has a δ-function singularity (in numerical terms a conveniently characterised sharp peak) but of course $\rho_s(\underline{k}, \Omega)$ contains also additional information of interest.

Thus we have a formalism ready for doing practical calculations. The surface phonon band structure can be obtained either by looking for the roots of the secular equation, i.e., the determinant of (9.17), or else by looking for peaks in the spectral function (9.18). The latter, evaluated as a function of Ω for fixed $\underline{k}$, contains also spectral information of interest for all Ω, not only for the eigenvalues $\Omega(\underline{k})$, as will be seen in §11.

10. Examples of application

It is instructive to start with some academic example in order to get acquainted with the practical use of the formal analysis. Firstly we note the following point about (9.17): $\mathcal{J} \Phi_s G \mathcal{J}$ has layer matrix elements

$$\sum_{n \geq 0} \langle s | \Phi_s | n \rangle \langle n | G | s' \rangle = \langle s | \Phi_s G | s' \rangle \qquad (10.1)$$

if the crystal is contained in $\underline{n} \geq 0$, so that $\underline{n} = 0$ is the terminal surface layer. Remember that $\underline{s}$ spans the (surface) domain of $\mathcal{J}$. If this consists of only one atomic layer then the terms of Φ_s entering (10.1) can be pictured as

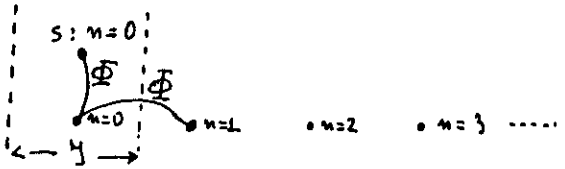

Then the sum of (10.1) includes $\underline{n} = 0$ (which is $\underline{s}$) and also $\underline{n} = 1$. But (31
$\mathcal{J}$ usually includes more than one atomic layer and in practice often just two. Then the picture is

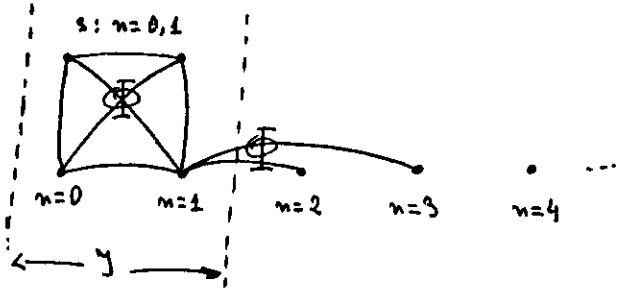

In this case $\underline{s}$ includes $\underline{n} = 0$ and $\underline{n} = 1$ and the sum of (10.1) includes up to $\underline{n} = 3$.

The elements $\langle s | \Phi_s | n \rangle$, for $\underline{n} \geq 0$, may or may not be equal to the same $\langle s | \Phi | n \rangle$ of the bulk crystal. They are for ideal cleavage. Otherwise we have some surface perturbations, $\Delta\Phi$, as stressed earlier. By definition $\Delta\Phi$ is all contained in $\mathcal{J}$, with matrix elements

$$(\mathcal{J} \Delta\Phi \mathcal{J})_{ss'} = \langle s | \Delta\Phi | s' \rangle . \qquad (10.2)$$

Then

$$\mathcal{J}\Phi_s G \mathcal{J} = \mathcal{J}\Phi G \mathcal{J} + \mathcal{J}\Delta\Phi\mathcal{J} G \mathcal{J} = \mathcal{J}\Phi G \mathcal{J} + \mathcal{J}\Delta\Phi\mathcal{J}\mathcal{J} G \mathcal{J} = \mathcal{J}\Phi G \mathcal{J} + \mathcal{J}\Delta\Phi\mathcal{J} \qquad (10.3)$$

and (9.17) reads

$$\mathcal{G}_s^{-1} = \mathcal{J}\Omega - \mathcal{J}\Phi G \mathcal{J} - \mathcal{J}\Delta\Phi\mathcal{J} \qquad (10.4)$$

For ideal cleavage ($\Delta\Phi = 0$), $\mathcal{G}_s^{-1}$ has the value that we may call 'unperturbed'

$$\mathcal{G}_{s0}^{-1} = \mathcal{J}\Omega - \mathcal{J}\Phi G \mathcal{J} \qquad (10.5)$$

and (10.4) reads

$$\mathcal{G}_s^{-1} = \mathcal{G}_{s0}^{-1} - \mathcal{J}\Delta\Phi\mathcal{J} , \qquad (10.6)$$

which is nothing but a Dyson equation in the $\mathcal{J}$ domain, where $\mathcal{J}\Delta\Phi\mathcal{J}$ is the perturbation.

It is clear that the hard labour lies in determining $\mathcal{G}_{s0}^{-1}$(10.5), which amounts to redoing the lattice dynamics for the half-crystal. We shall consider some examples of ideally cleaved surfaces, which suffice to acquire familiarity with the basic features involved in surface phonon calculations. Before doing this we note that the layer matrix elements of the terms $\mathcal{J}\Phi_s^0\mathcal{J}$ involve sums of the form

$$\langle s|\Phi_s^0|s'\rangle = \sum_{n\geq 0}{}' \langle s|\Phi|n\rangle\langle n|G|s'\rangle . \qquad (10.7)$$

The prime on Σ' indicates that <u>not all terms with n=0 enter in the definition</u> of this sum. The point is that Σ' includes only the interactions in the existing half of the crystal and leave out, by definition, those associated with the missing atoms. Imagine just a linear chain and a force term of the type

$$\sum_n \Phi_{0n} u_n = K(u_0-u_{-1})+K(u_0-u_1), \qquad (10.8)$$

corresponding simply to NN interactions.

If a surface is created at $n=0$, so that the half 'crystal' is in $n\geq 0$, then

$$\sum_{n\geq 0}{}' \Phi_{0n}u_n = \Phi_{00}'u_0+\Phi_{01}u_1 = K(u_0-u_1), \qquad (10.9)$$

i.e., Φ_{00} is actually $2K$, but Φ_{00}', which enters in $\Sigma'_{n\geq 0}$, is only K. The other contribution to Φ_{00} goes into the definition of the complementary sum

$$\sum_{n\leq 0}{}' \Phi_{0n}u_n = \bar{\Phi}_{00}'u_0+\Phi_{0,-1}u_{-1} = K(u_0-u_{-1}) . \qquad (10.10)$$

In 3-D the details are more complicated, but this example suffices to illustrate the idea. In 3-D the two sums are less symmetrical because $\Sigma'_{n\geq 0}$ <u>includes also by definition the interactions between atoms in the surface layers</u>, which are all excluded from $\Sigma'_{n\leq 0}$. For instance,

in 2-D with NN interactions $\Sigma'_{n\geq 0}$ includes interactions of the central

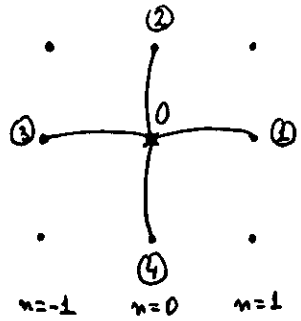

atom (0) under consideration with neighbours (1), (2) and (4), while $\Sigma'_{n\leq 0}$ includes only the interaction with neighbour (3). This can be used to simplify the secular equation in the following manner.

Consider the definition of G for the bulk crystal

$$(\Omega-\Phi)G = I \qquad (10.11)$$

Take the projection in the domain $\mathcal{J}$ which will become the surface domain when the surface is created by (in this case) ideal cleavage. Then

$$-\mathcal{J}\Phi G\mathcal{J} = \mathcal{J}-\Omega\mathcal{G} \qquad (10.12)$$

i.e.

$$-\sum_{n\geq 0}{}' \langle s|\Phi|n\rangle\langle n|G|s'\rangle = \langle s|(\mathcal{J}-\Omega\mathcal{G})|s'\rangle + \sum_{n\leq 0}{}' \langle s|\Phi|n\rangle\langle n|G|s'\rangle \qquad (10.13)$$

From (10.13) and (10.5) we have

$$\langle s|\mathcal{G}_{s0}^{-1}|s'\rangle = \langle s|\Omega_s\mathcal{G}^{-1}\Omega|s'\rangle + \sum_{n\leq 0}{}' \sum_{s''} \langle s|\Phi|n\rangle\langle n|G|s''\rangle\langle s''|\mathcal{G}^{-1}|s'\rangle \qquad (10.14)$$

i.e.

$$\mathcal{G}_{s0}^{-1} = (\mathcal{J}+\mathcal{J}\bar{\Phi}G\mathcal{J})\mathcal{G}^{-1} \qquad (10.15)$$

where

$$\langle s|\mathcal{J}\bar{\Phi}G\mathcal{J}|s'\rangle = \sum_{n\leq 0}{}' \langle s|\Phi|n\rangle\langle n|G|s'\rangle \qquad (10.16)$$

Thus the secular equation can be cast simply as

$$\det|\mathcal{J}+\mathcal{J}\bar{\Phi}G\mathcal{J}| = 0 \qquad (10.17)$$

instead of

$$\det|(10.5)| = \det|\mathcal{J}\Omega-\mathcal{J}\Phi G\mathcal{G}^{-1}| = 0 \qquad (10.18)$$

The algebra is simplified for two reasons: (i) $\mathcal{J}\bar{\Phi}G\mathcal{J}$ includes fewer terms than $\mathcal{J}\Phi_s^0 G\mathcal{J}$, as stressed above. (ii) We can omit the factor $\mathcal{G}^{-1}$. However, <u>this is necessary for the spectral function (9.18)</u>.

(34

We now take as an exercise Rosenzweig's model: Simple cubic lattice, central forces, NN interactions with force constant K and NNN interactions with force constant This is obtained from the model worked out in Appendix A by putting $K' = \frac{1}{2}K$ and $K'' = 0$. This simple model is isotropic in the long wave limit, which is a shortcoming, but it satisfies the condition of rotational invariance (5.5) and yields the Rayleigh mode in the long wave limit, a property not shared by all simple models which have been often used. It also has just sufficient complexity to exhibit one of the characteristic features of a 3-D crystal, namely, the appearance of 'windows' in the continuum obtained from the projection of the bulk band structure. In this case the surface domain consists of one atomic layer ($n = 0$). We must now be a bit more precise concerning notation. In the above equations we have emphasised only the layer index, but in 3-D we have the three labels (l_1, l_2, l_3), which we write as (l, m, n), as in Appendix A. We put $L = (l, m)$ and remember that Φ and G are 3×3 matrices. Thus for $\| \bar{\Phi} G \|$ we have to evaluate the sums

$$\sum_{\alpha\beta}(L, L') = \sum_{n \le 0}{}' \sum_{L} \sum_{\gamma} \langle L, 0 | \Phi_{\alpha\gamma} | L + \Lambda, n \rangle \langle L + \Lambda, n | G_{\gamma\beta} | L', 0 \rangle \qquad (10.19)$$

Λ is also a 2-D discrete label $(\Delta l, \Delta m)$ giving the 2-D position from the central atom $L = (l, m)$. It remains to define the surface orientation. We shall study the (0,0,1) surface, with (l, m, n) associated with (x, y, z). The Φ terms involved on (10.19) can be obtained from the results given in Appendix A, remembering that (u_x, u_y, u_z) are written as (u, v, w). The Λ's entering (10.19) are obtained by inspection of Fig. A.1. For instance, for $\langle L, 0 | (\bar{\Phi} G)_{x\beta} | L', 0 \rangle$ we start from $-F_x$ (with $K' = \frac{1}{2}K$ and $K'' = 0$) and identify the coefficients of all $\underline{u}$ terms. The coefficients thus obtained are to be multiplied by $G_{x\beta}$ terms. Then the coefficients of $\underline{v}$ terms contribute to Φ_{xy} terms, to be multiplied by $G_{y\beta}$ terms (as a matter of fact in this case this contribution is zero) and the coefficients of $\underline{w}$ terms contribute to Φ_{xz} terms, to be multiplied by $G_{z\beta}$ terms. The result is

(35

$$\langle L, 0 | (\bar{\Phi} G)_{x\beta} | L', 0 \rangle = -\frac{K}{2}\big[\langle L + (1,0), -1 | G_{x\beta} | L', 0 \rangle + \langle L + (\bar{1}, 0), -1 | G_{x\beta} | L', 0 \rangle - 2\langle L, 0 | G_{x\beta} | L', 0 \rangle + \langle L + (\bar{1}, 0), -1 | G_{z\beta} | L', 0 \rangle - \langle L + (1,0), -1 | G_{z\beta} | L', 0 \rangle\big] \qquad (10.20)$$

The other terms are likewise obtained.

Another technical point to note is that the first result which comes from the analysis depends on 2-D (discrete) position variables and we still have to perform the 2-D Fourier transform. We indicate the actual position vectors as $\underline{L} = (l, m)\,a$, etc. Take a matrix element $\langle L, n | G | L', n' \rangle$ with 2-D Fourier transform (ξ-dependence understood):

$$\langle n | G(\xi) | n' \rangle = \sum_{L, L'} e^{-i\underline{\xi}\cdot\underline{L}} \langle L, n | G | L', n' \rangle e^{i\underline{\xi}\cdot\underline{L}'}. \qquad (10.21)$$

Then the 2-D Fourier transform of $\langle L + \Lambda, n | G | L', n' \rangle$ is

$$e^{i\underline{\xi}\cdot\underline{\Lambda}} \langle n | G(\xi) | n' \rangle. \qquad (10.22)$$

This holds for functions, like the $G_{\alpha\beta}$'s, which depend only on the difference $\underline{L} - \underline{L}'$. Thus, for the evaluation of (10.20) it suffices to evaluate the transform of $\langle L, n | G | L', 0 \rangle$ for $n = 0, -1$ and to use (10.22). For instance, for ξ in the (1,0,0) direction and putting $\varphi = ak$ we find the terms listed in Appendix B. Note that the (xy), (yx), (yz) and (zy) elements of $\langle 0 | (\bar{\Phi} G)_{x\beta} | 0 \rangle$ vanish. Finally we obtain

$$\zeta_{so}^{-1} = \begin{Vmatrix} \frac{D_{xx}}{D} & 0 & \frac{D_{xz}}{D} \\ 0 & \frac{D_{yy}}{\langle 0|G_{yy}|0\rangle} & 0 \\ \frac{D_{zx}}{D} & 0 & \frac{D_{zz}}{D} \end{Vmatrix} \qquad (10.23)$$

The various D's are listed in Appendix B and the G's for this model are easily evaluated. We have included the factor ζ^{-1} because we want to see (below) all effects contained in the spectral function (9.18).

Now, recall the discussion in §6 where we saw that in cubic materials, for propagation in the (1,0,0) direction of the (0,0,1) surface, there is a decoupling of a shear horizontal mode (degenerate with the bulk threshold) and a surface sagittal mode with amplitudes $(u_x, 0, u_z)$. This feature is not restricted to the long wave limit. It is a consequence of the cubic symmetry which shows up again in the form of (10.23). The (yy) term yields the transverse shear horizontal mode and the rest is a (2×2) determinant with sagittal polarisation. Fig. 10 shows the projection of the bulk bands for this model and surface orientation, as well as the surface modes resulting from (10.23). These include the Rayleigh mode, below the lowest bulk threshold, and another branch appearing in the window which opens up inside the projection of the bulk continuum. Now take a given value of κ corresponding to $\varphi = a\kappa = 0.63\pi$ (for the vector $\underline{\xi}$ in this direction this is something like the point $\bar{\Sigma}$ of Fig. 9) and cut vertically across the bands shown in Fig. 10. Consider the spectral function $\rho_s(\underline{\xi}, \Omega)$ (9.19). For fixed $\underline{\xi}$ this gives the surface projection as a function of the frequency variable Ω which runs along the corresponding vertical line. The most significant values correspond to the points labelled (1)

to (6) in Fig. 10. Actually we change from $\Omega = m\omega^2$ to ω, so ρ_s becomes $\rho_s(\underline{\xi}, \omega)$, as discussed in §8. Fig. 11 gives the corresponding spectral function exhibiting the two surface modes and the bulk threshold effects.

This is a very simple model but in essence the above exercise demonstrates the kind of analysis involved in real surface phonon calculations and the results exhibit many of the characteristic features of real crystals, including anti-resonance. In §4 we saw the details of another simple example, namely, an f.c.c. lattice with central force NN interactions. This is not only an academic model but also one which, used with caution, may have some reasonable practical value. From a rigorous point of view the important role played by d-electrons in a metal like, e.g., Ni would require for a microscopic calculation a nondiagonal dielectric matrix, a proper treatment of anisotropic ionic potentials and a calculation altogether very complicated indeed. However, this simple force constants model actually yields a not unreasonable picture of bulk surface phonons in Ni [16]. We shall consider it here as a working tool to study surfaces of f.c.c. metals. There has been considerable experimental activity producing metal surface phonon data from inelastic atom scattering [17-21] and electron energy loss spectroscopy [22], although the interpretation of the latter type of experimental data tends to be rather more involved.

A calculation of surface phonon dispersion relations for the Ni-(0,0,1) surface can be carried out by following the same pattern as expounded above for Rosenzweig's model and using the results for the bulk dynamics seen in §4. For this surface the $\underline{x}, \underline{y}, \underline{z}$ axes are the (1,0,0), (0,1,0) and (0,0,1) symmetry axes. The primitive translation vectors can be taken as

$$\underline{t}_1 = \frac{a}{2}(1,1,0)\ ;\ \underline{t}_2 = \frac{a}{2}(1,\bar{1},0)\ ;\ \underline{t}_3 = \frac{a}{2}(0,0,1) \qquad (10.24)$$

with associated 2-D reciprocal lattice vectors

$$\underline{g}_1 = 2\pi \frac{\underline{t}_2 \wedge \underline{t}_3}{\underline{t}_1 \cdot (\underline{t}_2 \wedge \underline{t}_3)} = \frac{2\pi}{a}(1,1,0)\ ;\ \underline{g}_2 = 2\pi \frac{\underline{t}_3 \wedge \underline{t}_1}{\underline{t}_2 \cdot (\underline{t}_3 \wedge \underline{t}_1)} = \frac{2\pi}{a}(1,\bar{1},0)\,. \qquad (10.25)$$

The 2-D Brillouin Zone is inserted in Fig. 12, which shows the calculated [23] surface phonon dispersion relations for Ni-(0,0,1) when the tip of $\underline{k}$ spans the lines $\bar{\Gamma}\bar{M}$, $\bar{M}\bar{X}$ and $\bar{\Gamma}\bar{X}$ of the said 2-D B.Z. Note the usual Rayleigh mode (S_1), the modes S_6 and S_7 appearing in the windows of the projection of the bulk bands (compare with Fig. 10 for a simple cubic lattice) and the S_4 mode which starts out as a sharp resonance just above the lower transverse bulk threshold and eventually (near the B.Z. boundary at $\bar{X}$) becomes a distinct surface mode again. This model contains one parameter which was adjusted to fit the maximum bulk frequency. The results are very similar to those obtained in other calculations [24,25]. The S_4 mode has been experimentally found [25] and the overall agreement is quite reasonable considering the extreme simplicity of the model. A considerably better agreement of course is obtained with a more elaborate model [26] involving central and angular forces with up to NNN interactions. On the other hand it can be argued that the failure of the simple calculation to follow the downward bending of this phonon branch near the B.Z. edge is mainly due to the assumption of ideally unrelaxed surface, a deficiency which is easily remedied. An inward relaxation of the surface relaxation resulting in a 20% increase in the force constant parameter between the first and second atomic layers appears to be

capable of accounting for this bending [25]. Thus it is reasonable to say that between some elaboration of the model - mainly inclusion of three body forces - and some relaxation of the surface layer one can have a rather reliable picture.

A little more complete are the experimental data [21] on Ag-(1,1,1), another f.c.c. metal. We can also try to study this in terms of the same simple model. The geometry for this surface is different. For this we rotate the $\underline{x}, \underline{y}, \underline{z}$ axes to $\underline{x}', \underline{y}', \underline{z}'$ in the directions $(1,1,\bar{2})$, $(\bar{1},1,0)$, $(1,1,1)$ - always the $\underline{z}$ axis perpendicular to the surface. The primitive lattice translations can then be chosen as

$$\underline{t}_1 = \left(\frac{a}{\sqrt{2}}, 0, 0\right),\ \underline{t}_2 = \left(\frac{-a}{\sqrt{8}}, \frac{3a}{\sqrt{24}}, 0\right),\ \underline{t}_3 = (0,0,a) \qquad (10.26)$$

with 2-D reciprocal lattice vectors

$$\underline{g}_1 = \frac{\sqrt{2}\pi}{a}\left(1, \frac{1}{\sqrt{3}}, 0\right),\ \underline{g}_2 = \frac{\sqrt{8}\pi}{a}\left(0, \frac{2}{\sqrt{3}}, 0\right)\,. \qquad (10.27)$$

The 2-D B.Z. is shown in Fig. 13, which also shows the experimental data [21] and the results of a calculation [23] carried out by using again the same method and model as for Ni-(0,0,1) and fitting the one force constant parameter to the maximum bulk frequency [27]. Only distinct surface states were sought in this calculation. The resulting dispersion curves for this Rayleigh-type mode are in close agreement with those obtained in other calculations for the same type of model [24,28]. Experimental evidence shows in this case another mode in the $\bar{\Gamma}\bar{M}$ and $\bar{\Gamma}\bar{K}$ directions. These are resonance branches which one could also obtain by looking for complex eigenvalues of the secular equation (10.17) or (10.18) or by studying the spectral function $\rho_s(\underline{k},\Omega)$ (9.19)

for fixed $\underline{k}$ as a function of Ω and looking for a second peak above the Rayleigh peak. But again the ideal surface calculation does not follow the downward bending of the experimental branches near the B.Z. boundaries. This is also well reproduced by combining a more elaborate model with some changes in the surface force constants [12]. It is not unlikely that just the latter, even with the simple model, could yield a reasonable fit to experimental data, but these are detailed technicalities which do not concern us here. The most relevant feature of this case is the appearance of distinctly identifiable resonance branches.

11. Surface phonon spectra and inelastic atom-surface scattering data

Although it has been known for quite some time that inelastic atom scattering off solid surfaces could constitute a desirable spectroscopic method to study surface phonons and the theoretical foundation existed already in the late sixties [29, 30] it has not been until the eighties that sufficient resolution has been achieved [21, 31] so that this has become a very useful experimental research tool capable of producing good surface phonon spectra. Basically the method works better for low excitation energies because at higher energies (say, optical phonon frequencies in ionic crystals) multiphonon processes might be involved, rendering the interpretation of experimental data more too clear. Yet the first important experiments of this kind have been done mainly with ionic crystals, as the acoustic mode region of these involves lower frequencies than that of, say, metals. More recently the technique has been considerably improved and even optical mode can also be detected [32].

In an elementary analysis of ionic crystal dynamics one assumes rigid ion displacements but recognises that these entail (in the optical modes) dipole moments and associated electric fields. The rigid-ion lattice polarisability thus enters the lattice dynamics of ionic crystals in the usual manner explained in textbooks. The idea of the shell models [33] is to introduce a new concept, namely, that the ions are not rigid. The positive ion core is assumed to be rigid but the electronic charge around it is deformable, i.e., the ions themselves are also polarisable. These deformations entail at least another contribution to the dipole moment, with associated electric field, and this is then included in the lattice dynamics so that this now involves the ionic polarisability. In the simplest approximation within a shell model one considers a bodily displacement of the electronic charge, undeformed, relative to the positive ion core. This is sufficient to produce a dipole. In the next step, called the breathing shell model, one assumes also radial deformations of the electronic charge such that only dipolar deformations are involved. This suffices to introduce sufficient anisotropy that Cauchy's relations do not hold in the long wave limit. Of course one could go on and allow also for quadrupole deformations. This would surely amount to some improvement, but in practice the breathing shell model involving only dipolar deformations appear to work so well that it is profusely used with good results for the lattice dynamics of ionic crystals.

Green functions can also be used to study (bulk or) surface lattice dynamics in different ways. There is one, called Invariant Green Function (IGF) method [36] which is especially useful to study

surface lattice dynamics of ionic crystals. In this method one starts formally from a slab but eventually lets it thickness tend to infinity so that the two surfaces are completely decoupled, but this is a mere technicality. The idea is to describe the introduction of the surface as a perturbation of the bulk crystal (which leads to work in the restricted localised space of the surface domain) and to impose the conditions that the force constants for both the complete and the incomplete crystal must satisfy translational (and parallel to the surface) as well as rotational invariance. Thus the terms of the perturbation which creates the surface must also satisfy the same invariance conditions. This is expressed by means of a projection on the surface domain and this is the way to express the surface (boundary) conditions. The term <u>perturbation</u> has here only a formal meaning. It does not imply solving the problem by some approximation scheme. We are back to the idea of studying the surface problem by using only the projection in the localised surface domain and doing there all the algebra. In this analysis [34] the layer description of the crystal is carried out in such a way that the long range Coulomb interactions are summed by layers and one is left with effective interlayer interactions which decay very fast with distance. This makes the IGF method very useful to study ionic crystal surfaces. Combined with the breathing shell model it has produced very useful results in practice.

Fig. 14 shows the results of such a calculation [34] for LiF(0,0,1) in excellent overall agreement with experimental data except for one significant detail. The data near the B.Z. edge again bend downwards below the theoretical (broken line) curve for ideal surface. The same behaviour as that of the broken line of Fig 14 was found earlier in slab calculations [24].

The breathing shell model is here very useful in helping to understand the situation. An adjustment of the polarisability of the bulk F^- ions gives already a better result (heavy line), but a 17% increase of the polarisability of the surface F^- ions is still needed to obtain a perfect agreement [35]. A detailed study shows that in LiF for the Rayleigh modes near the B.Z. edge it is mainly the anions that move and thus their polarisability is important in determining the outcome. NaF is different in that for the same type of Rayleigh modes (near $\bar{M}$) the anions are at rest, while they move in the modes of the optical branches (for long waves these are referred to as Lucas modes [36]). Owing to their larger size, the anions usually interact more strongly with the incident He atoms used in the experiment and so it has become possible to detect the optical surface modes in NaF(0,0,1) by inelastic atom scattering, as shown in Fig. 15. The results are also in very good agreement with IGF calculations based on the breathing shell model [31].

It is clear that the IGF method and the method described in §§ 9,10 have many features in common. Both use Green functions, both deal with the surface as a distinct problem and in both one ends up by projecting in the localised surface domain, so that the information on the bulk crystal is embodied in its corresponding bulk G, but only the surface projection (ζ in §§ 9,10) is used to study surface phonons. In practical terms, the secular matrix is never larger than necessary and in both cases the size of its matrix is the same. Moreover, it can be proved [37] that although the two methods are differently originated and they have a different scope, in the part where they overlap they are identically equivalent.

More precisely, the object called G_s in §§ 9.10, i.e., the surface projection of the Green function of the semiinfinite crystal, is identically the object called g_s in the IGF method. Moreover, in one method one is led naturally to G_s^{-1} and in the other one one is led naturally to g_s^{-1} and the reason is that this is precisely the secular matrix. But the interesting thing is that this object, G_s or g_s, contains more information than just the surface phonon eigenvalues, as we stressed earlier. For fixed $\underline{K}$ the secular equation yields the surface eigenfrequencies, but $G_s(\underline{K},\Omega)$, or $g_s(\underline{K},\Omega)$, studied as a function of Ω yields the spectral function $\rho_s(\underline{K},\Omega)$ (9.19) which, as we saw, is the local value for fixed $\underline{K}$ of the projected mode density for the terminal atomic layer.

What makes this particularly interesting is that this is precisely what is involved in the interpretation of inelastic atom scattering spectra. Let us translate ρ_s into $\rho_s(\underline{K},\omega)$. In the experiments, $\hbar\underline{K}$ is the momentum parallel to the surface exchanged between incident atom (the probe) and semiinfinite crystal (the target) and one makes an energy analysis: $\hbar\omega$ is the energy exchanged and the experiment yields the inelastic scattering cross section $\sigma(\underline{K},\omega)$ as a function of ω for fixed $\underline{K}$. The detailed analysis requires some care and some labour, as surface modes may be <u>created</u> or <u>annihilated</u>, and the scattering may be <u>backward</u> or <u>forward</u>, but such details are outside our scope. What is relevant from our point of view is the conspicuous role played by $\rho_s(\underline{K},\omega)$. In any study of this problem there are three distinct ingredients. One is the model used for the interaction between incident atom and surface atoms. The second one is the approximations

made in formulating and solving the scattering problem itself. These aspects are discussed in another course in this College. The third ingredient is the description of the spectrum of surface modes created or absorbed. Without going into the details of this analysis it is clear that $\sigma(\underline{K},\omega)$ is going to be essentially proportional to $\rho_s(\underline{K},\omega)$, since σ essentially maps out the spectral density of the modes involved in the process. We can also look at it in this way: The cross section is ultimately proportional to the mean square value of the vibrating amplitudes at the surface, $\langle u_s^2\rangle$, which is classically the size of the obstacle with which the incoming atom collides. More technically, this is to be Fourier analysed so it is a function of $(\underline{K},\omega)$. Now, $\langle u_s^2\rangle$ is a (surface) autocorrelation function. In general fluctuation-dissipation theory, via thermal average, etc. the autocorrelation function is in the end proportional to the imaginary part of the corresponding response function, which in this case is just G_s. Thus we expect that σ is essentially proportional to $\mathrm{Im}\,\mathrm{tr}\,G_s$, i.e. to ρ_s. The trace is due to the fact that we must add up the contributions from all possible polarisations.

The interchangeability between the two Green function methods just commented provides a very convenient scheme, as formulae from either method can be combined in practice to obtain $\rho_s(\underline{K},\omega)$. Fig. 16 shows experimental results for LiF-(0,0,1) and theoretical results obtained in this way [37]. Three different calculations are presented. They differ in the atom-atom potentials and in the approximations used to solve the scattering problem but all three use the same $\rho_s(\underline{K},\omega)$ obtained in the manner indicated above and based on a breathing shell model (actually

weighted by Bose-Einstein and Debye-Waller factors which a complete analysis requires). The point is that the details vary, of course, but the key features of the spectrum remain and are in good agreement with experiment. This demonstrates how important it is to have a reliable description of surface phonon dynamics for the analysis of inelastic atom scattering spectra. It also bears out the observation anticipated in §6 and evident also in Brillouin scattering data (Fig. 6) that when the surface modes are excited (or absorbed) it is the entire surface dynamics that is excited (or absorbed), not only the surface modes.

Further details on atom-surface scattering are outside the scope of these notes. They will be covered in another course in this College and can also be found in [38], where plenty of information related to surface lattice dynamics is contained.

REFERENCES

A) GENERAL BACKGROUND REFERENCES. BULK

- P. Brüesch, 'Phonons: Theory and experiment I. Lattice dynamics and models of interatomic forces' (Springer, 1982).
  Very good for physical models.
- J.W. Cochran, 'The dynamics of atoms in crystals' (E. Arnold, Ltd., London, 1973).
  Also very intuitive and good for physical models, although less up to date and more restricted in scope than Brüesch.
- G.W. Leibfried, 'Lattice dynamics', in Theory of condensed matter, ICTP International College, 1967, p. 175 (International Atomic Energy Agency, Vienna 1968).
  A good general introduction. Authoritative pedagogic presentation

of general principles. Formal aspects made easy.

- A.A. Maradudin, E.W. Montroll, G.H. Weiss and I.P. Ipatova, 'Theory of lattice dynamics in the harmonic approximation'. Supplement 3 of the series Solid State Physics (H. Ehrenreich, F. Seitz and D. Turnbull, edits. Academic Press 1971)
  Formal and advanced aspects. For professionals. Contains also a chapter on surfaces.
- Also many standard textbooks on physics of solids contain general treatments of bulk lattice dynamics at different levels to suit all tastes.

B. GENERAL BACKGROUND REFERENCES. SURFACE.

- G.W. Farnell, 'Properties of elastic surface waves', in Physical Acoustics, Vol VII (W.P. Mason edit., Academic Press, 1969).
  Rather extensive and dealing exclusively with long wave (elastic wave) limit. Formulation based on traditional matching method. Contains a great deal of information
- F. García-Moliner, 'Theory of surface waves', in Crystalline semiconducting materials and devices, p. 483. ICTP International College, 1984 (P.N. Butcher, N.H. March and M.P. Tosi, edits. Plenum Press, 1986).
  Less extensive and more didactically oriented than Farnell. Deals also exclusively with long wave limit. Formulation based on Surface Green Function Matching method.
- A.A. Maradudin, R.F. Wallis and L. Dobrzynski, 'Surface phonons and polaritons'. Handbook of surfaces and interfaces. Vol 3. (Garland STPM Press, New York, 1980).
  Very extensive. Elastic waves and, mostly, discrete lattice phonons. Treats

in detail formal aspects of surface lattice dynamics.

- G. Benedek, 'Dynamics of solid surfaces'. Physicalia Magazine, Vol 7, Suppl. 1 (1985).

General and authoritative account of the state of the art up to 1985. Physicalia Magazine is published by the Belgian Physical Society, Boeretang 200, 2400 Mol, Belgium.

C. SPECIFIC REFERENCES QUOTED IN THE TEXT.

[1] See Farnell in general references B

[2] J. R. Sandercock, Solid State Commun. 26 (1978) 547.

[3] V.R. Velasco and F. García-Moliner, Surf. Sci. 143 (1984) 93.

[4] See García-Moliner in general references B.

[5] V.R. Velasco and F. García-Moliner, J. Phys. C: Solid State Phys. 13 (1980) 2237.

[6] W. Kress, F.W. deWolfe, A.D. Kulkarni and U. Schröder. Phys. Rev. B 35 (1987) 5783.

[7] See Maradudin, Wallis and Dobrzynski in general references B.

[8] V.R. Velasco and F. Yndurain, Surf. Sci. 85 (1979) 107.

[9] A. Fasolino, G. Santoro and E. Tosatti, Phys. Rev. Lett. 44 (1980) 1684.

[10] G. Armand, Solid St. Commun. 48 (1983) 261.

[11] T.S. Rahman, J.E. Black and D.L. Mills, Phys. Rev. B 25 (1982) 883.

[12] V. Bortolani, A. Franchini, F. Nizzoli and G. Santoro, Phys. Rev. Lett. 52 (1984) 429.

[13] J. Szefter and A. Khater, J. Phys. C: Solid St. Physics (1987)

[14] F. García-Moliner, G. Platero and V.R. Velasco, Surf. Sci. 136 (1984) 601.

[15] F. García-Moliner and V.R. Velasco, Progr. Surf. Sci. 21 (1986) 93. (Pergamon Press, S.G. Davison edit.)

[16] L.V. Heimendal and M.F. Thorpe, J. Phys. F: Metal Phys. 5 (1975) L 87.

[17] S.C. Yerkes and D.R. Miller, J. Vac. Sci. Technol. 17 (1980) 126.

[18] B.F. Mason and B.R. Williams, Phys. Rev. Lett. 46 (1981) 1138.

[19] M. Cates and D.R. Miller, Proc. Int. Conf on Vibrations at Surfaces, Asilomar, California, Aug. 1982.

[20] B. Feuerbacher and R.F. Willis, Phys. Rev. Lett. 47 (1981) 526.

[21] R.B. Doak, U. Harten and J.P. Toennies, Phys. Rev. Lett. 51 (1983) 578.

[22] J.M. Szeftel, S. Lehwald, H. Ibach, T.S. Rahman and D.L. Mills, Phys. Rev. Lett 51 (1983) 268.

[23] G. Platero, V.R. Velasco and F. García-Moliner, Surf. Sci. 152/153 (1985) 819.

[24] R.E. Allen, G.P. Alldredge and F.W. deWette, Phys. Rev. B 4 (1971) 1661.

[25] S. Lehwald, J.M. Szeftel, H. Ibach, T.S. Rahman and D.L. Mills, Phys. Rev. Lett. 50 (1983) 518.

[26] V. Bortolani et al., in 'Dynamics of gas-surface interactions'. G. Benedek and U. Valbusa edits. (Springer, Heidelberg 1982).

[27] V. Bortolani, A. Franchini, F. Nizzoli, G. Santoro, G. Benedek, V. Celli and N. Garcia. Solid St. Commun. 48 (1983) 1045.

[28] G. Armand, Solid St. Commun. 48 (1983) 261.

[29] N. Cabrera, V. Celli and R. Manson. Phys. Rev. Lett. 22 (1969) 346.

[30] R. Manson and V. Celli Surf. Sci. 24 (1971) 495.

[31] G. Brusdeylins, R.B. Doak and J.P. Toennies, Phys. Rev. B 27 (1983) 3662.

[32] G. Brusdeylins, R. Rechsteiner, J.G. Skofronick, J.P. Toennies, G. Benedek and L. Miglio, Phys. Rev. Lett. 54 (1985) 466.

[33] See Brüesch in general references A.

[34] G. Benedek, Surf. Sci. 61 (1976) 603.

[35] G. Benedek, P. Brivio, L. Miglio and V.R. Velasco, Phys. Rev. B 26 (1982) 487.

[36] A.A. Lucas, J. Chem. Phys. 48 (1968) 3156.

[37] G. Platero, V.R. Velasco, F. García-Moliner, G. Benedek and L. Miglio, Surf. Sci. 148 (1984) 243

[38] 'Dynamics of gas-surface interaction', G. Benedek and U. Valbusa, edits (Springer, Heidelberg, 1982).

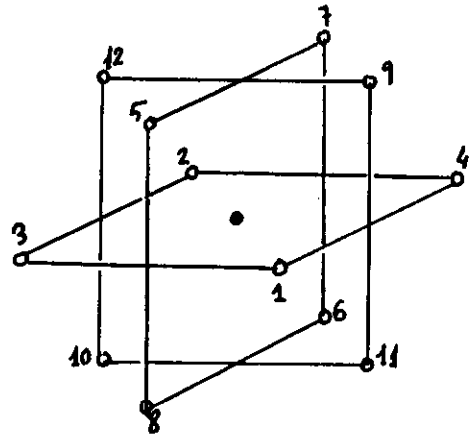

Fig. 1. F.c.c. lattice. One atom (•), taken as central atom, surrounded by 12 NN (○) labelled 1 to 12. The unit vectors going from the central atom to each one of the NN are $\underset{\sim}{r}_{0j} = \frac{1}{\sqrt{2}}(L^0_{j1}, L^0_{j2}, L^0_{j3})$. We list $(L^0_{j1}, L^0_{j2}, L^0_{j3})$ for all 12 cases:

(1): $(1,1,0)$	(5): $(1,0,1)$	(9): $(0,1,1)$
(2): $(\bar{1},\bar{1},0)$	(6): $(\bar{1},0,\bar{1})$	(10): $(0,\bar{1},\bar{1})$
(3): $(1,\bar{1},0)$	(7): $(\bar{1},0,1)$	(11): $(0,1,\bar{1})$
(4): $(\bar{1},1,0)$	(8): $(1,0,\bar{1})$	(12): $(0,\bar{1},1)$

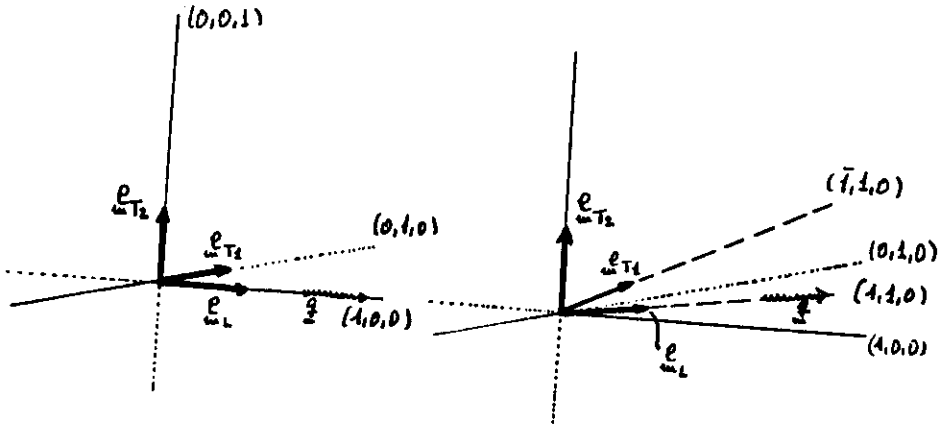

Fig 2. Cubic symmetry. ~~~: Propagation vector ⟶: Polarisation vector

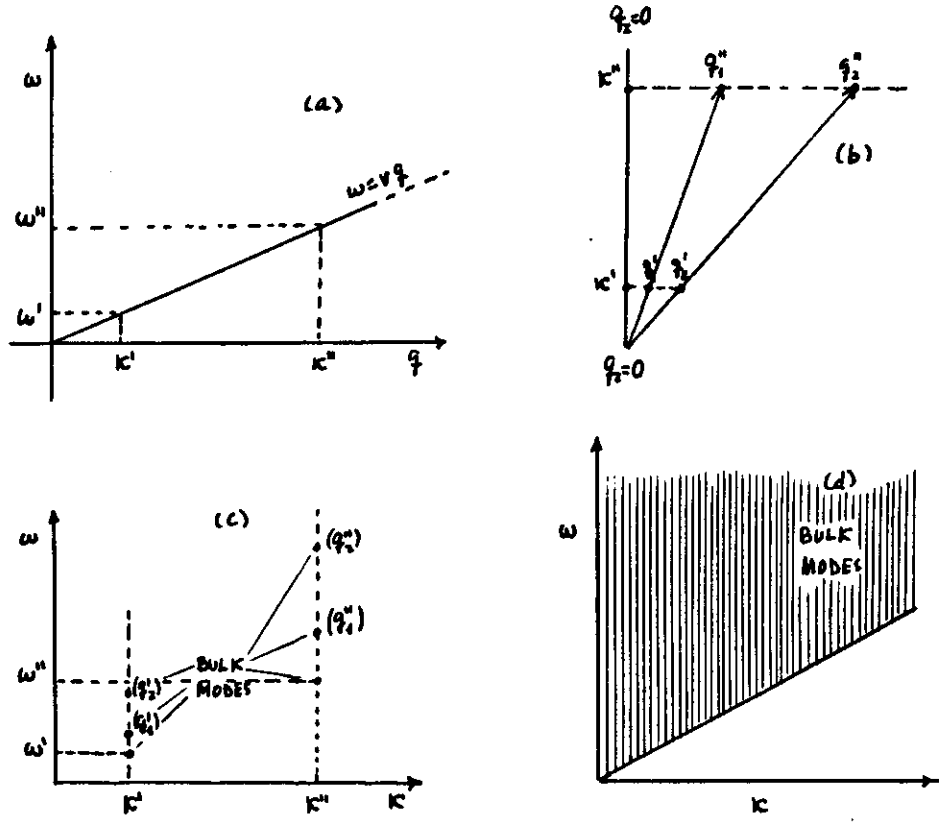

Fig 3. Elastic continuum. Projection of bulk modes.

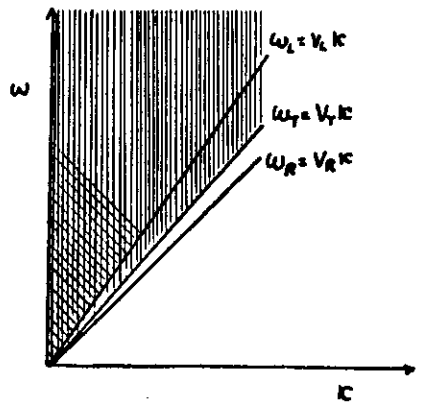

Fig 4. Projection of the bulk modes and surface (Rayleigh) mode for isotropic elastic medium.

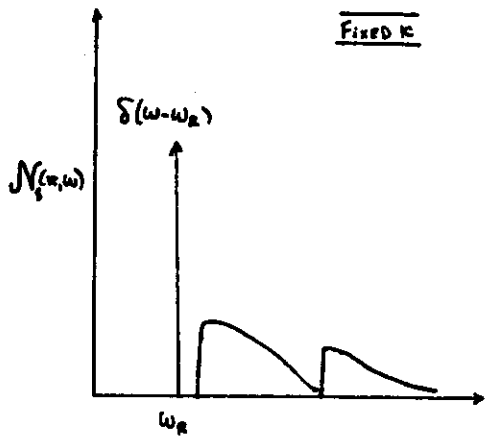

Fig 5. Qualitative form of the surface projected, fixed κ mode density for an elastic isotropic medium.

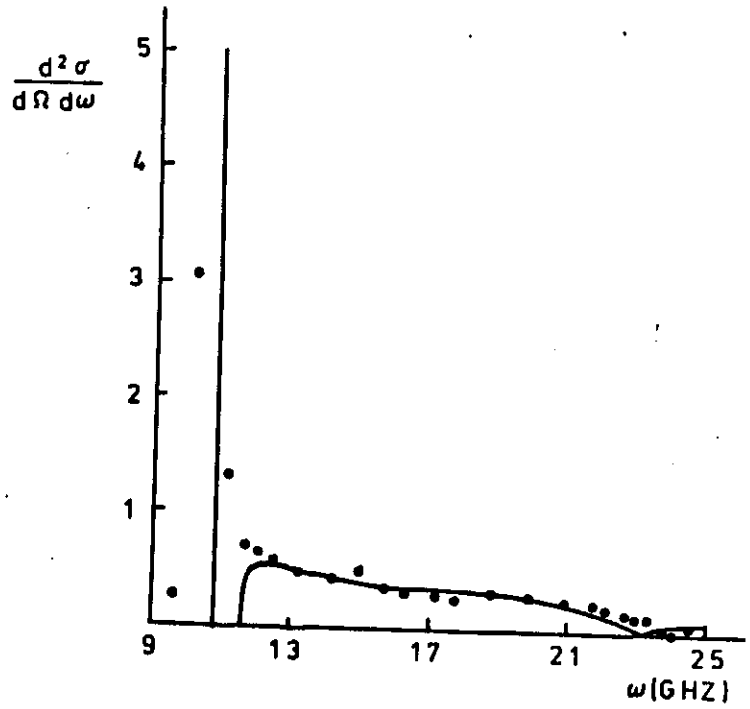

Fig. 6. Dots: Experimental [2] surface Brillouin scattering data for polycrystalline Al. Continuous lines: Surface Green function matching calculation [3] of the surface projection of the fixed κ mode density. Calculated for an isotropic average of elastic (long wave) Al with κ corresponding to the experiment.

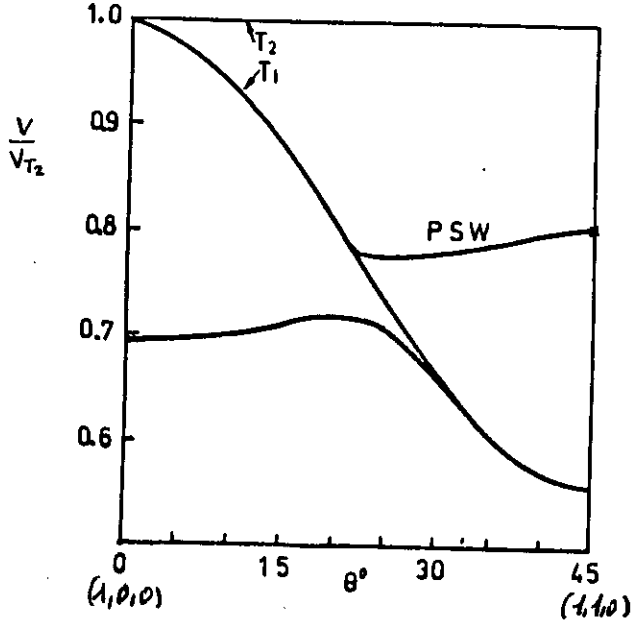

Fig.8. Cubic elastic medium. (0,0,1) surface. Variation of bulk transverse threshold and surface wavephase velocities for different propagation directions. The actual results correspond to Cu.

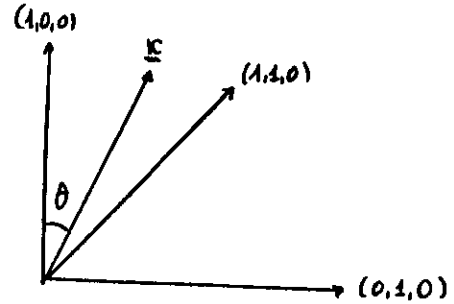

Fig.7. Defining θ for Fig.8

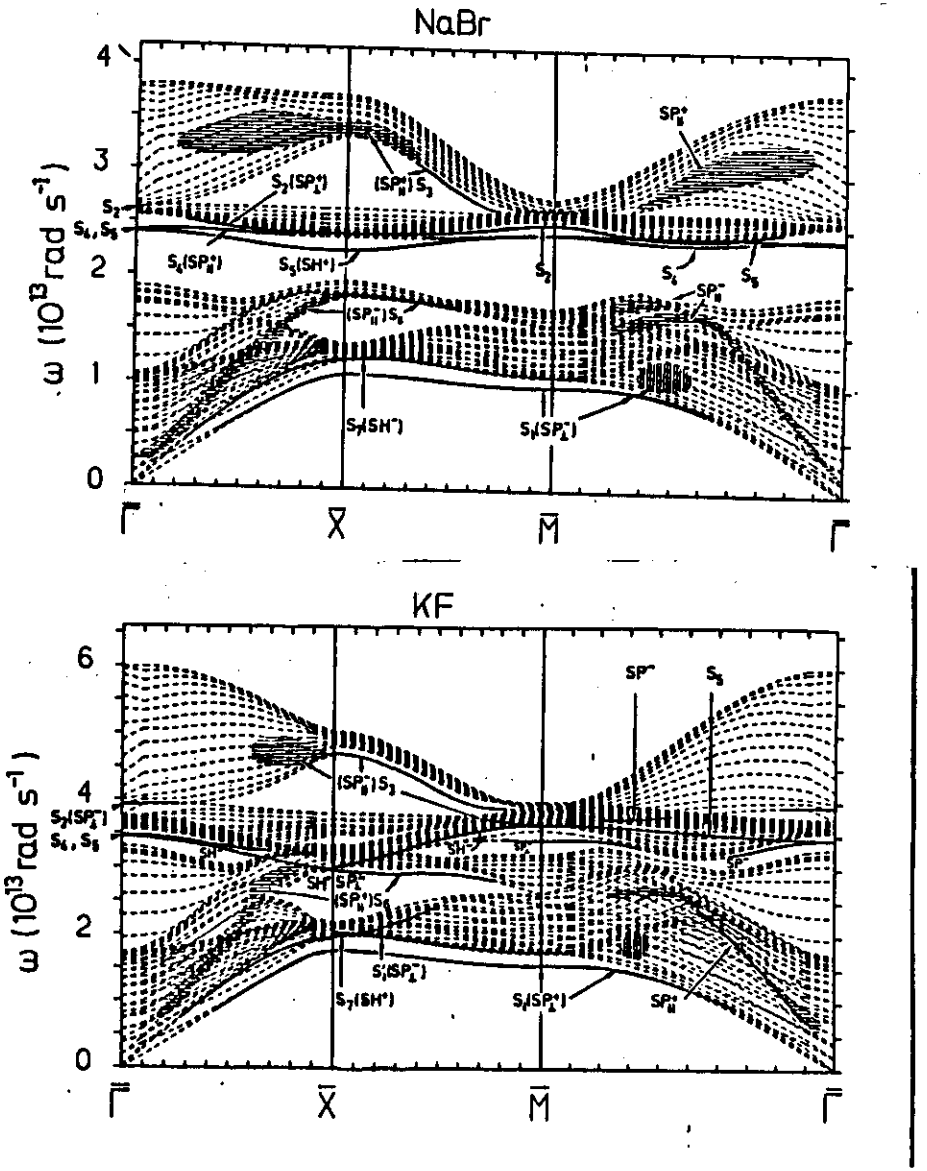

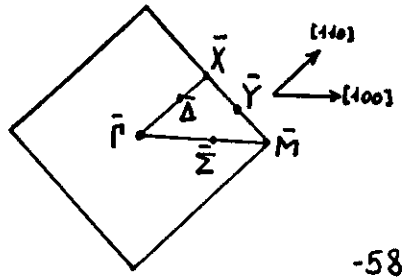

Fig.9. Slab calculation [6] of surface phonon dispersion relations with corresponding projection - (0,0,1) surface - of the bulk bands. Shown below is the 2-D Brillouin zone for this surface

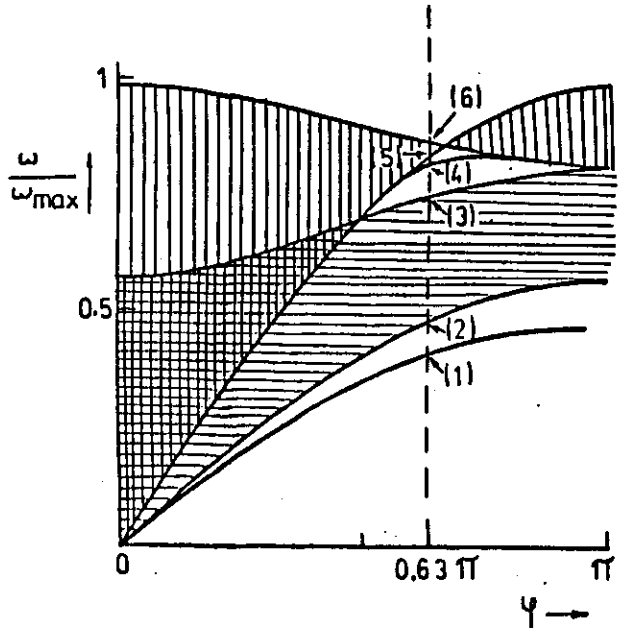

Fig. 10. Rosenzweig's model. (0,0,1) surface. $\underline{\kappa} = \kappa(1,0,0)$. $\varphi = a\kappa$. Projection of bulk bands and surface modes.

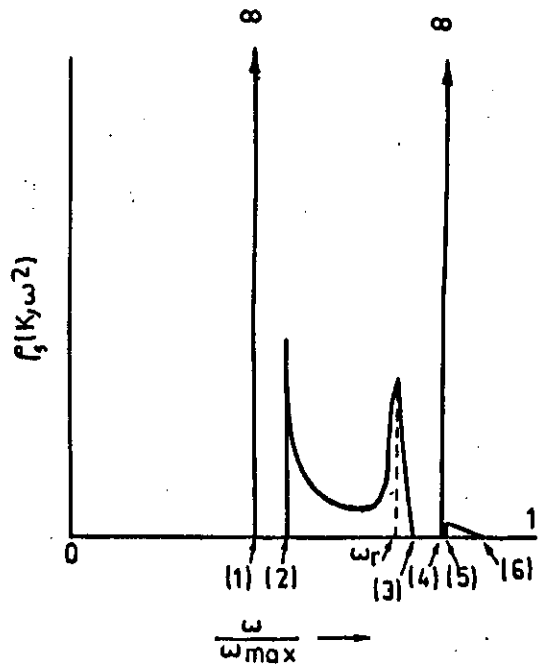

Fig 11. Local value, projected at the surface, of the fixed κ mode density for the same situation as that of Fig. 10. The points labelled (1) to (6) correspond to those shown in Fig. 10. Note the δ-function peaks for surface states, bulk threshold effects and a resonance (ω_r) near the bulk threshold (3).

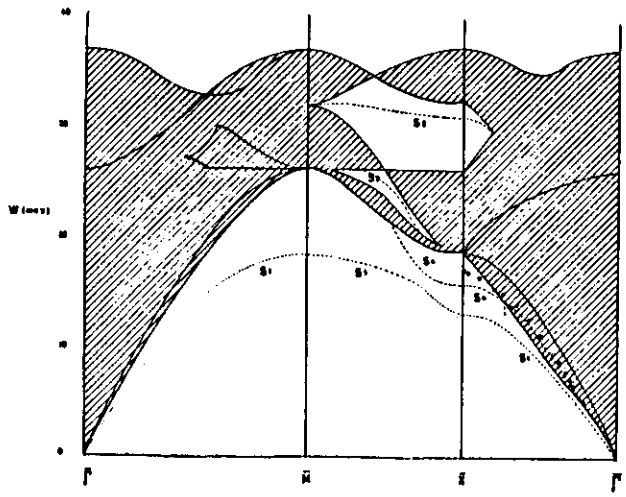

Fig. 12. Projected bulk bands and calculated [23] and measured [25] surface phonon bands for Ni-(0,0,1). The calculation was done for an ideal, unrelaxed surface. The corresponding 2-D Brillouin zone appears in Fig. 9.

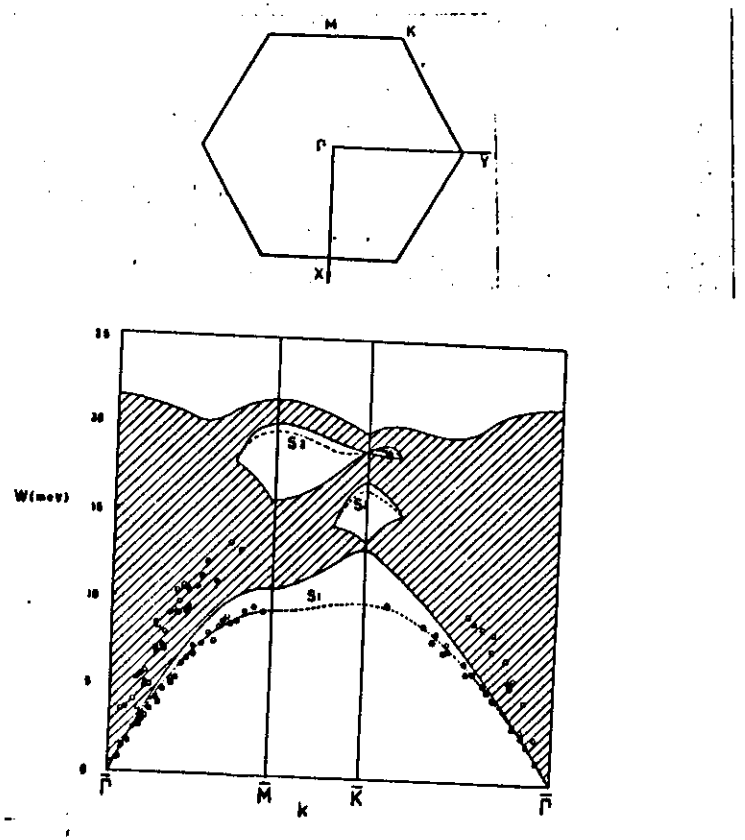

Fig. 13. Same as Fig. 12 for Ag-(111). The calculation was set up only distinct (real eigenvalue) surface modes. Shown above is the corresponding 2-D Brillouin zone.

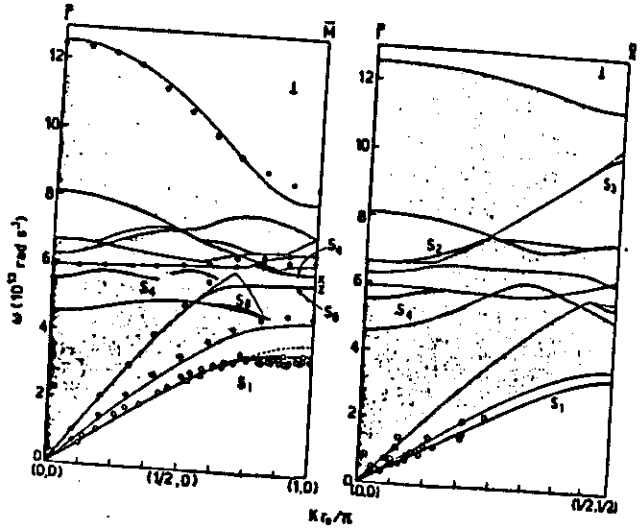

Fig. 14. Li-(0,0,1). Projected bulk bands and surface phonon bands. Discussion in the text.

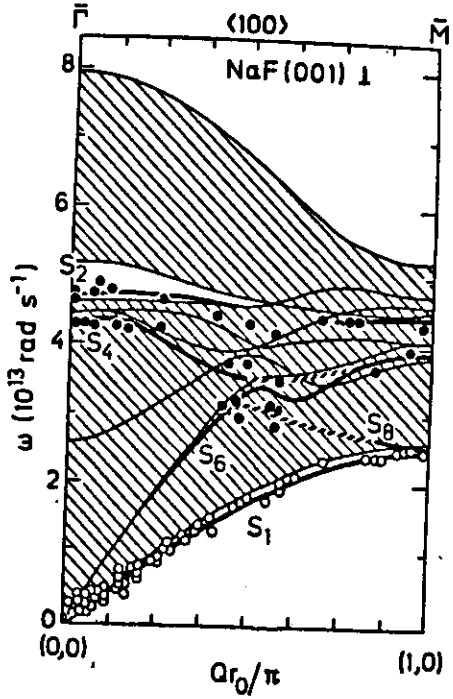

Fig. 15. Same as Fig. 14, for NaF(0,0,1)

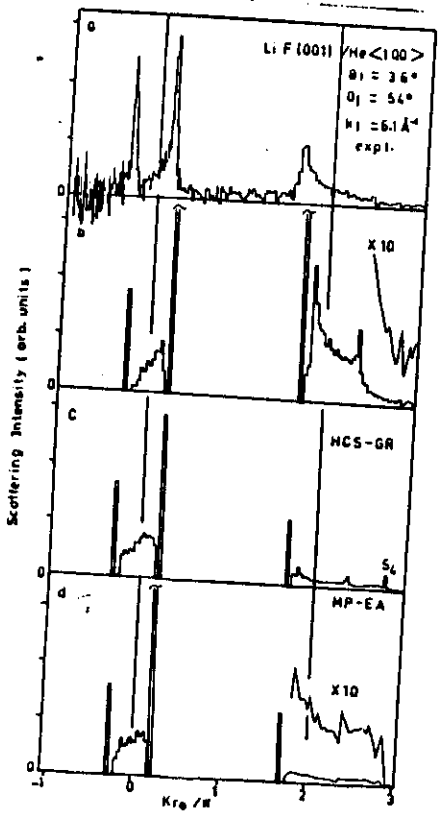

Fig. 16 Experimental and theoretical inelastic scattering cross section for fixed κ as a function of energy for LiF-(0,0,1). Kr_0/π is a measure of the energy change of the reflected atoms. Discussion in the text.

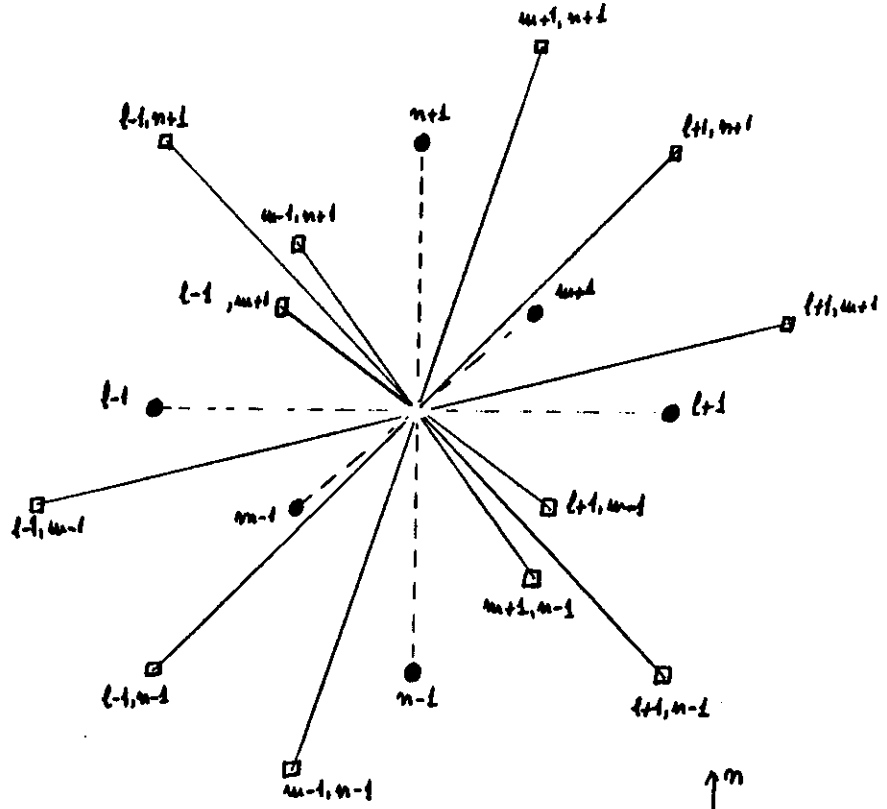

Simple cubic lattice
Central atom l, m, n
NN: Nearest neighbours (6) : ●
NNN: Next nearest neighbours (12): □
Position labels not explicitly shown are l, m or n
e.g: Central atom is (l, m, n)
l+1, m+1 is (l+1, m, n+1)

Fig A. 1

Appendix A: Force constants and equations of motion for a simple cubic lattice with NN and NNN interactions and central and angular forces

This was first used for a model calculation by D.C. Gazis, R. Herman and R.F. Wallis, Phys. Rev. 119 (1960) 533. It is instructive to carry out the full exercise by starting from the starting of the physical model and working out the force constants and equations of motion. The geometrical details are shown on Fig. A.1. We simplify the notation and use (l,m,n) instead of (l_1,l_2,l_3), in this case associated with (x,y,z). We also write (u,v,w) instead of (u_x,u_y,u_z). Now for the various terms. We view atomic positions and displacements from the n (or z, or $0,0,\underline{1}$) axis:

Central forces: The contributions to Φ^{NN} which originate central forces acting on the central atom under consideration, (l,m,n) are due to:

(i) 

u displacements from atoms with the same (m,n)

(ii) 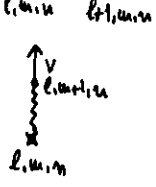

v " " " " " " (l,n)

(iii) 

w " " " " " " (l,m)

Thus
$$\Phi^{NN}_{central} = K\left[(u_{l,m,n}-u_{l+1,m,n})^2+(u_{l,m,n}-u_{l-1,m,n})^2\right.$$
$$+(v_{l,m,n}-v_{l,m+1,n})^2+(v_{l,m,n}-v_{l,m-1,n})^2 \qquad (A.1)$$
$$\left.+(w_{l,m,n}-w_{l,m,n+1})^2+(w_{l,m,n}-w_{l,m,n-1})^2\right].$$

K is one of the parameters of the model. Note that a displacement perpendicular to the line joining two atoms also contributes to central forces (the spring is also stretched as the distance varies). However, consider the

following picture: 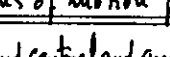

For small displacements:

$\frac{\delta a}{a_0} = \frac{(a_0^2+v^2)^{1/2}-a_0}{a_0} \simeq \frac{1}{2}\left(\frac{v}{a_0}\right)^2$, which gives a contribution to Φ of order $\left(\frac{\delta a}{a_0}\right)^2 \propto \left(\frac{v}{a_0}\right)^4$, i.e., a higher order term beyond the harmonic approximation. The force terms derived from A.1 and acting in the x direction is

$$-F^{NN}_{x,central} = 2K\left[(u_{l,m,n}-u_{l+1,m,n})+(u_{l,m,n}-u_{l-1,m,n})\right] \qquad (A.2)$$

We now indicate by ${}^{l}\Phi^{NNN}_{central}$, ${}^{m}\Phi^{NNN}_{central}$, ${}^{n}\Phi^{NNN}_{central}$ the contributions to $\Phi_{central}$ coming from NNN atoms contained in the planes $\underline{l}$ = const, $\underline{m}$ = const, $\underline{n}$ = const., respectively. Then

$$
\begin{aligned}
{}^{n}\Phi^{NNN}_{central} = K'\Big\{&\left[(u_{l,m,n}+v_{l,m,n})-(u_{l+1,m+1,n}+v_{l+1,m+1,n})\right]^2\\
&+\left[(u_{l,m,n}+v_{l,m,n})-(u_{l-1,m-1,n}+v_{l-1,m-1,n})\right]^2\\
&+\left[(u_{l,m,n}-v_{l,m,n})-(u_{l+1,m-1,n}-v_{l+1,m-1,n})\right]^2\\
&+\left[(u_{l,m,n}-v_{l,m,n})-(u_{l-1,m+1,n}-v_{l-1,m+1,n})\right]^2,
\end{aligned}
\qquad (A.3)
$$

whence the contribution to F_x:

$$
\begin{aligned}
-{}^{n}F^{NNN}_{x,central} = 2K'\Big\{&\left[(u_{l,m,n}+v_{l,m,n})-(u_{l+1,m+1,n}+v_{l+1,m+1,n})\right]+\left[(u_{l,m,n}+v_{l,m,n})-(u_{l-1,m-1,n}+v_{l-1,m-1,n})\right]\\
&+\left[(u_{l,m,n}-v_{l,m,n})-(u_{l+1,m-1,n}-v_{l+1,m-1,n})\right]+\left[(u_{l,m,n}-v_{l,m,n})-(u_{l-1,m+1,n}-v_{l-1,m+1,n})\right]
\end{aligned}
\qquad (A.4)
$$

K' is another parameter of the model. Likewise we find

$$
\begin{aligned}
-{}^{m}F^{NNN}_{x,central} = 2K'\Big\{&\left[(u_{l,m,n}+w_{l,m,n})-(u_{l+1,m,n+1}+w_{l+1,m,n+1})\right]+\left[(u_{l,m,n}+w_{l,m,n})-(u_{l-1,m,n-1}+w_{l-1,m,n-1})\right]\\
&+\left[(u_{l,m,n}-w_{l,m,n})-(u_{l+1,m,n-1}-w_{l+1,m,n-1})\right]+\left[(u_{l,m,n}-w_{l,m,n})-(u_{l-1,m,n+1}-w_{l-1,m,n+1})\right]
\end{aligned}
\qquad (A.5)
$$

It is easily seen that ${}^{\ell}F^{NNN}_{x,\text{central}} = 0$ because ${}^{\ell}\Phi^{NNN}_{\text{central}}$ involves only v's and w's, but not u's. We have obtained all contributions to $F_{x,\text{central}}$, whence the total force, including NN and NNN interactions. Knowing F_x we obtain F_y and F_z by appropriate cyclic permutations.

Angular bending forces: We use the same sort of notation, which should be selfexplanatory. The different contributions are as follows.

(i) 

$${}^{n}\Phi_{(i)} = K''\left[(u_{\ell,m+1,n} - u_{\ell,m,n}) + (V_{\ell+1,m,n} - V_{\ell,m,n})\right]^2 \qquad (A.6)$$

$$-{}^{n}F_x^{(i)} = -2K''\left[(u_{\ell,m+1,n} - u_{\ell,m,n}) + (V_{\ell+1,m,n} - V_{\ell,m,n})\right] \qquad (A.7)$$

(ii) 

$$-{}^{n}F_x^{(ii)} = -2K''\left[(u_{\ell,m+1,n} - u_{\ell,m,n}) - (V_{\ell-1,m,n} - V_{\ell,m,n})\right] \qquad (A.8)$$

(iii) 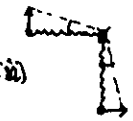

$$-{}^{n}F_x^{(iii)} = -2K''\left[(u_{\ell,m+1,n} - u_{\ell,m,n}) + (V_{\ell-1,m,n} - V_{\ell,m,n})\right] \qquad (A.9)$$

(iv) 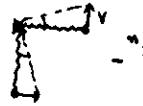

$$-{}^{n}F_x^{(iv)} = -2K''\left[(u_{\ell,m-1,n} - u_{\ell,m,n}) - (V_{\ell,m+1,n} - V_{\ell,m,n})\right] \qquad (A.10)$$

(v) 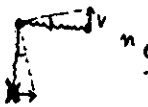

$${}^{n}\Phi^{(v)} = K''\left[(u_{\ell,m,n} - u_{\ell,m+1,n}) - (V_{\ell+1,m,n} - V_{\ell,m+1,n})\right]^2 \qquad (A.11)$$

$$-{}^{n}F_x^{(v)} = 2K''\left[(u_{\ell,m,n} - u_{\ell,m+1,n}) - (V_{\ell+1,m,n} - V_{\ell,m+1,n})\right] \qquad (A.12)$$

(vi) 

$${}^{n}\Phi^{(vi)} = K''\left[(u_{\ell,m,n} - u_{\ell,m-1,n}) + (V_{\ell+1,m-1,n} - V_{\ell,m-1,n})\right]^2 \qquad (A.13)$$

$$-{}^{n}F_x^{(vi)} = 2K''\left[(u_{\ell,m,n} - u_{\ell,m-1,n}) + (V_{\ell+1,m,n} - V_{\ell,m-1,n})\right] \qquad (A.14)$$

(vii) 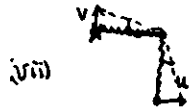

$${}^{n}\Phi^{(vii)} = K''\left[(u_{\ell+1,m-1,n} - u_{\ell+1,m,n}) + (V_{\ell,m,n} - V_{\ell+1,m,n})\right]^2 \qquad (A.15)$$

$$-{}^{n}F_x^{(vii)} = 0 \qquad (A.16)$$

(viii) 

$${}^{n}\Phi^{(viii)} = K''\left[(u_{\ell-1,m-1,n} - u_{\ell,m-1,n}) - (V_{\ell,m,n} - V_{\ell-1,m,n})\right]^2 \qquad (A.17)$$

$$-{}^{n}F_x^{(viii)} = 0 \qquad (A.18)$$

(ix) 

$${}^{n}\Phi^{(ix)} = K''\left[(u_{\ell+1,m+1,n} - u_{\ell+1,m,n}) + (V_{\ell,m+1,n} - V_{\ell+1,m,n})\right]^2 \qquad (A.19)$$

$$-{}^{n}F_x^{(ix)} = 0 \qquad (A.20)$$

(x) 

$${}^{n}\Phi^{(x)} = K''\left[(u_{\ell+1,m+1,n} - u_{\ell+1,m,n}) - (V_{\ell,m+1,n} - V_{\ell+1,m+1,n})\right]^2 \qquad (A.21)$$

$$-{}^{n}F_x^{(x)} = 0 \qquad (A.22)$$

(xi) 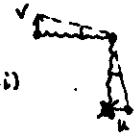

$${}^{n}\Phi^{(xi)} = K''\left[(u_{\ell,m+1,n} - u_{\ell,m+1,n}) - (V_{\ell-1,m+1,n} - V_{\ell,m+1,n})\right]^2 \qquad (A.23)$$

$$-{}^{n}F_x^{(xi)} = 2K''\left[(u_{\ell,m+1,n} - u_{\ell,m+1,n}) - (V_{\ell-1,m+1,n} - V_{\ell,m+1,n})\right] \qquad (A.24)$$

(xii) 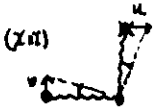

$${}^{n}\Phi^{(xii)} = K''\left[(u_{\ell,m,n} - u_{\ell,m-1,n}) - (V_{\ell-1,m-1,n} - V_{\ell,m-1,n})\right]^2 \qquad (A.25)$$

$$-{}^{n}F_x^{(xii)} = 2K''\left[(u_{\ell,m,n} - u_{\ell,m-1,n}) - (V_{\ell+1,m-1,n} - V_{\ell,m-1,n})\right] \qquad (A.26)$$

Then the total

$${}^{n}F_{x,\text{ang}} = \sum_{(v)\pm(i),\ldots,(xii)} {}^{n}F_x^{(v)} \qquad (A.27)$$

${}^{n}F_{x,\text{ang}}$ is obtained from ${}^{n}F_{x,\text{ang}}$ by changing $\begin{cases} V \to W \\ u_{n+\varepsilon} \to u_{n+\varepsilon} \\ n \to m \end{cases}$ $(\varepsilon = \pm 1)$

${}^{\ell}F_{x,\text{ang}} = 0$ ($u_{\ell,m,n}$ does not enter ${}^{\ell}\Phi^{\text{ang}}$)

With this we can write down the equation of motion for $u_{\ell,m,n}$. Some cancellations among the above contributions take place on adding up and then

$$M\ddot{u}_{\ell,m,n} = 2K[u_{\ell+1,m,n}+u_{\ell-1,m,n}-2u_{\ell,m,n}] \quad \text{central, NN}$$

$$+2K'[u_{\ell+1,m+1,n}+u_{\ell-1,m-1,n}+u_{\ell+1,m-1,n}+u_{\ell-1,m+1,n}+u_{\ell,m,n+1}+u_{\ell,m,n-1}+u_{\ell+1,m,n-1}+u_{\ell-1,m,n+1}-8u_{\ell,m,n}] \quad \text{central, NNN}$$

$$* \quad +2K'[V_{\ell+1,m+1,n}+V_{\ell-1,m-1,n}-V_{\ell+1,m-1,n}-V_{\ell-1,m+1,n}+W_{\ell+1,m,n+1}+W_{\ell-1,m,n-1}-W_{\ell+1,m,n-1}-W_{\ell-1,m,n+1}] \quad \text{central NNN}$$

$$** \quad +2K''[V_{\ell+1,m+1,n}+V_{\ell-1,m-1,n}-V_{\ell+1,m-1,n}-V_{\ell-1,m+1,n}+W_{\ell+1,m,n+1}+W_{\ell-1,m,n-1}-W_{\ell+1,m,n-1}-W_{\ell-1,m,n+1}] \quad \text{angular}$$

$$+8K''[u_{\ell,m+1,n}+u_{\ell,m-1,n}+u_{\ell,m,n+1}+u_{\ell,m,n-1}-4u_{\ell,m,n}] \quad \text{angular} \qquad (A.28)$$

Note *, **: Identical form. Different physical origin.

$M\ddot{v}_{\ell,m,n}$ and $M\ddot{w}_{\ell,m,n}$ are obtained from (A.28) by cyclic permutation of (u,v,w) and of the increments $\delta = \pm 1$, $\varepsilon = \pm 1$ on the indices ℓ, m, n.

E.g. for $M\ddot{v}_{\ell,m,n}$: $\begin{matrix} u \\ v \\ w \end{matrix} \to \begin{matrix} v \\ w \\ u \end{matrix}$ and

$$\begin{matrix} \ell+\delta \\ m \\ n \end{matrix} \to \begin{matrix} \ell \\ m+\delta \\ n \end{matrix}; \quad \begin{matrix} \ell+\delta \\ m+\varepsilon \\ n \end{matrix} \to \begin{matrix} \ell \\ m+\delta \\ n+\varepsilon \end{matrix}; \quad \begin{matrix} \ell+\delta \\ m \\ n+\varepsilon \end{matrix} \to \begin{matrix} \ell+\varepsilon \\ m+\delta \\ n \end{matrix}; \quad \begin{matrix} \ell \\ m+\delta \\ n \end{matrix} \to \begin{matrix} \ell \\ m \\ n+\delta \end{matrix} \to \begin{matrix} \ell+\delta \\ m \\ n \end{matrix}$$

For this one can cast (A.28) in the equivalent condensed form

$$M\ddot{u}_{\ell,m,n} = 2K\Big\{\sum_{\delta=\pm1}(u_{\ell+\delta,m,n}-u_{\ell,m,n})\Big\}+2K'\Big\{\sum_{\delta=\pm1}\sum_{\varepsilon=\pm1}(u_{\ell+\delta,m+\varepsilon,n}+u_{\ell+\delta,m,n+\varepsilon}-2u_{\ell,m,n})\Big\} \qquad (A.29)$$

$$+2(K'+K'')\Big\{\sum_{\delta=\pm1}\sum_{\varepsilon=\pm1}[\varepsilon\delta(V_{\ell+\delta,m+\varepsilon,n}+W_{\ell+\delta,m,n+\varepsilon})\Big\}+8K''\Big\{\sum_{\delta=\pm1}(u_{\ell,m+\delta,n}+u_{\ell,m,n+\delta}-2u_{\ell,m,n})\Big\}$$

In the elastic limit

$$a c_{11} = 2(K+4K')$$
$$a c_{12} = 4K' \qquad (A.30)$$
$$a c_{44} = 2(2K'+K'')$$

$c_{11} \neq c_{12}+2c_{44}$ (anisotropic). Cauchy's relations not obeyed

For $K''=0$ (central forces only) the long wave limit yields an elastic isotropic medium with $c_{11} = c_{12}+2c_{44}$ (Cauchy's relations)

Appendix B: Simple cubic lattice with central force NN and NNN interactions. Rosenszweig's model.

We give here some results for $\underline{k}$ in the (1,0,0) direction in layer notation for (0,0,1) layers. Layer index n. $\varphi = ak$. We put

$$\bar{\Sigma}_{\alpha\beta} = \langle 0|(\bar{\Phi}G)_{\alpha\beta}|0\rangle \qquad (B.1)$$

This is the $\underline{k}$-dependent 2-D Fourier transform of $\langle L,0|(\bar{\Phi}G)_{\alpha\beta}|L',0\rangle$ for $\underline{k} = (\kappa,0,0)$. Ω-dependence is understood throughout. The terms $\langle n|G_{\alpha\beta}|n'\rangle$ are likewise the 2-D Fourier transforms of $\langle L,n|G_{\alpha\beta}|L',n'\rangle$. The property (10.22) has been used and the $\bar{\Sigma}'_s$ are

$$\bar{\Sigma}_{xy} = \bar{\Sigma}_{yx} = \bar{\Sigma}_{yz} = \bar{\Sigma}_{zy} = 0 \qquad (B.2)$$

$$\bar{\Sigma}_{xx} = K[-\cos\varphi\langle -1|G_{xx}|0\rangle + \langle 0|G_{xx}|0\rangle + i\sin\varphi\langle -1|G_{xz}|0\rangle] \qquad (B.3)$$

$$\bar{\Sigma}_{xz} = K[-\cos\varphi\langle -1|G_{xz}|0\rangle + i\sin\varphi\langle -1|G_{zz}|0\rangle] \qquad (B.4)$$

$$\bar{\Sigma}_{zx} = K[-(2+\cos\varphi)\langle -1|G_{zx}|0\rangle + i\sin\varphi\langle -1|G_{xx}|0\rangle] \qquad (B.5)$$

$$\bar{\Sigma}_{zz} = K[-(2+\cos\varphi)\langle -1|G_{zz}|0\rangle + 3\langle 0|G_{zz}|0\rangle + i\sin\varphi\langle -1|G_{xz}|0\rangle] \qquad (B.6)$$

$$\bar{\Sigma}_{yy} = K[\langle 0|G_{yy}|0\rangle - \langle -1|G_{yy}|0\rangle] \qquad (B.7)$$

The terms entering (10.23) are

$$D_{xx} = \{1-K[-\cos\varphi\langle -1|G_{xx}|0\rangle + \langle 0|G_{xx}|0\rangle + i\sin\varphi\langle -1|G_{zx}|0\rangle]\}\langle 0|G_{zz}|0\rangle \qquad (B.8)$$

$$D_{xz} = -K[-\cos\varphi\langle -1|G_{xz}|0\rangle + i\sin\varphi\langle -1|G_{zz}|0\rangle]\langle 0|G_{xz}|0\rangle \qquad (B.9)$$

$$D_{zx} = K[-(2+\cos\varphi)\langle -1|G_{zx}|0\rangle + i\sin\varphi\langle -1|G_{xx}|0\rangle]\langle 0|G_{zz}|0\rangle \qquad (B.10)$$

$$D_{zz} = K\{1-K[-(2+\cos\varphi)\langle -1|G_{zz}|0\rangle + 3\langle 0|G_{zz}|0\rangle + i\sin\varphi\langle -1|G_{zz}|0\rangle\}\langle 0|G_{xx}|0\rangle \qquad (B.11)$$

$$D_{yy} = 1-K[-\langle -1|G_{yy}|0\rangle + \langle 0|G_{yy}|0\rangle] \qquad (B.12)$$

and $$D = \langle 0|G_{xx}|0\rangle\langle 0|G_{zz}|0\rangle - \langle 0|G_{zx}|0\rangle\langle 0|G_{xz}|0\rangle \qquad (B.13)$$

The matrix elements $G_{\alpha\beta}$ for this simple model are easily obtained by direct evaluation of the spectral representation

$$\langle n|\, G_{\alpha\beta}\, |n'\rangle = \frac{1}{2\pi} \sum_j \int_{-\pi}^{\pi} d\psi \lim_{\varepsilon\to 0} \frac{e_\alpha(\psi|j)\, e_\beta^*(\psi|j)\, e^{i\psi(n-n')}}{\omega_j(\psi) - \Omega + i\varepsilon} \qquad (B.14)$$

Here $\psi = a q_z$ and j labels the different eigenvalues and eigenvectors obtained from the dynamical matrix as explained in the text.

This is not always the most practical way to evaluate Green functions but it is the most direct one when the model is, as in this case, sufficiently simple that it can be worked out analytically.